Aus dem Institut für Klinische Neuroimmunologie
Klinikum der Ludwig-Maximilians-Universität München
Direktor: Prof. Dr. Martin Kerschensteiner

Die Optische Kohärenztomographie als moderne Methode zur Diagnose und Verlaufsbeurteilung von Neurodegeneration

Dissertation
zum Erwerb des Doktorgrades der Medizin
an der Medizinischen Fakultät der
Ludwig-Maximilians-Universität München

vorgelegt von
Luise Böhm

aus
Gießen

Jahr
2025

Mit Genehmigung der Medizinischen Fakultät der
Ludwig-Maximilians-Universität zu München

Erster Gutachter:	Prof. Dr. med. Tania Kümpfel
Zweiter Gutachter:	Prof. Dr. med. Ingo Kleiter
Dritter Gutachter:	Prof. Dr. med. Aljoscha Neubauer

Dekan:	Prof. Dr. med. Thomas Gudermann
Tag der mündlichen Prüfung:	06.02.2025

1. Affidavit

Eidesstattliche Versicherung

Böhm, Luise

Name, Vorname

Ich erkläre hiermit an Eides statt, dass ich die vorliegende Dissertation mit dem Titel:

Die Optische Kohärenztomographie als moderne Methode zur Diagnose und Verlaufsbeurteilung von Neurodegeneration

selbständig verfasst, mich außer der angegebenen keiner weiteren Hilfsmittel bedient und alle Erkenntnisse, die aus dem Schrifttum ganz oder annähernd übernommen sind, als solche kenntlich gemacht und nach ihrer Herkunft unter Bezeichnung der Fundstelle einzeln nachgewiesen habe.

Ich erkläre des Weiteren, dass die hier vorgelegte Dissertation nicht in gleicher oder in ähnlicher Form bei einer anderen Stelle zur Erlangung eines akademischen Grades eingereicht wurde.

München, 10.03.2025 _____Luise Böhm_____

Ort, Datum Unterschrift Doktorandin bzw. Doktorand

Inhaltsverzeichnis

2. Abkürzungsverzeichnis

BH_4 ..... *Tetrahydrobiopterin*
DMT.....*Disease Modifying Therapy*
EDSS .....*Expanded Disability Status Scale*
ETPKU.....*Early Treated Phenylketonuria*
FS .....*Funktionsscore*
GCIPL ..... *Kombinierte Ganglienzellschicht und Innere Plexiforme Zellschicht*
INL .....*Innere Körnerzellschicht*
KIS .....*Klinisch isoliertes Syndrom*
KUM .....*Klinikum Universität München*
MRT.....*Magnetresonanztomographie*
MS ..... *Multiple Sklerose*
MSK .....*Marianne-Strauss Klinik*
NEDA .....*no evidence of disease activity*
OCT.....*Optische Kohärenztomographie*
ON ..... *Optikusneuritis*
PAH..... *Phenylalaninhydroxylase*
PAH-Defizienz .....*Phenylalaninhydroxylase-Defizienz*
PIRA .....*progression independent of disease activity*
PKU .....*Phenylketonurie*
PPMS ..... *primär progrediente Multiple Sklerose*
PwPPMS..... *Personen mit primär progredienter Multiplen Sklerose*
RAW.....*relapse associated Worsening*
RIS ..... *Radiologisch isoliertes Syndrom*
RRMS .....*schubförmig remittierende Multiple Sklerose*
SPMS..... *sekundär progrediente Multiple Sklerose*
TMV ..... *Totales Makulavolumen*

3. Publikationsliste

Veröffentlichung I

Gernert JA*, Böhm L*, Starck M, Buchka S, Kümpfel T, Kleiter I, Havla J. **Inner Retinal Layer Changes Reflect Changes in Ambulation Score in Patients with Primary Progressive Multiple Sclerosis**. Int J Mol Sci. 2023 Aug 17;24(16):12872. doi: 10.3390/ijms241612872. PMID: 37629053; PMCID: PMC10454007.

Geteile Erstautorenschaft

Veröffentlichung II

Lotz-Havla AS, Weiß K, Schiergens K, Regenauer-Vandewiele S, Parhofer KG, Christmann T, Böhm L, Havla J*, Maier EM*. **Optical Coherence Tomography to Assess Neurodegeneration in Phenylalanine Hydroxylase Deficiency.** Front Neurol. 2021 Dec 10;12:780624. doi: 10.3389/fneur.2021.780624. PMID: 34956063; PMCID: PMC8703042.

Ko-Autorenschaft

Veröffentlichung III (außerhalb der vereinbarten Doktorarbeit zusätzlich entstanden)

Mulazzani E, Böhm L, Christmann T, Krumbholz M, Kümpfel T, Havla J. **Optical coherence tomography assessment of disease activity in cryopyrin-associated periodic syndrome**. Eur J Neurol. 2024 Apr 16:e16301. doi: 10.1111/ene.16301. Epub ahead of print. PMID: 38628041.

Ko-Autorenschaft

4. Einleitung

4.1 Hintergrund

Der Bedarf an individuellen Biomarkern zur differentialdiagnostischen Einordnung, Therapieentscheidung sowie zum Therapiemonitoring entzündlicher Erkrankungen des ZNS ist groß.[1]

Insbesondere die Multiple Sklerose (MS) ist geprägt von Neurodegeneration und Neuroinflammation und in ihrem klinischen, sowie paraklinischen Verlauf, sehr variabel.

Neben der Kernspintomographie (MRT) gibt es bislang jedoch nur wenige etablierte bildgebende Marker des Erkrankungsverlaufes, insbesondere für die progredienten Phasen der Multiplen Sklerose. [2] Der Einsatz der MRT ist aufgrund begrenzter Ressourcen jedoch limitiert. Aber auch andere Biomarker, die beispielsweise durch invasive Untersuchungen, wie die Liquorpunktion erhoben werden, sind nur eingeschränkt als Verlaufsmarker verfügbar.[3, 4]

Ziel eines neuen Markers ist, dass dieser valide, reliabel, nicht-invasiv, kosteneffektiv und gut reproduzierbar ist. Außerdem sollte er allgemein verfügbar sein. Idealerweise sollte der Marker sowohl Neurodegeneration als auch Neuroinflammation messen und damit helfen, die limitierten MRT-Ressourcen besser verwenden zu können. Einen möglichen alternativen Marker für Neurodegeneration und Neuroinflammation stellt die Optische Kohärenztomographie (OCT) für die retinale Bildgebung dar. [5] Die OCT nutzt die Tatsache, dass die Retina entwicklungsgeschichtlich Teil des Gehirns ist. Die Augen stülpen sich in der Embryogenese als zwei Bläschen aus dem Neuralrohr vor. Die Anlage der Retina geht damit aus dem neuronalen Gewebe hervor, somit entspricht die Netzhaut in Struktur und Aufbau dem Neurokortex. [6, 7] Damit kann man annehmen, dass durch die Vermessung der retinalen Schichtdicken ein „Blick ins Gehirn“ geworfen und gleichermaßen Neurodegeneration, aber auch Neuroinflammation sichtbar gemacht werden kann.

In den letzten Jahren konnte beispielhaft an der MS gezeigt werden, dass es zu retinalen Volumen- oder Dickeveränderungen nach einer Optikusneuritis, aber auch unabhängig von Schubereignissen, kommt. Diese messbaren Veränderungen korrelieren sowohl mit dem Hochkontrastvisus als auch mit der visuellen Wahrnehmungsqualität, welche sich direkt auf die

Lebensqualität auswirkt.[8] Auch konnte eine Assoziation mit klinischen Parametern, wie der Behinderungsprogression, bei Personen mit schubförmiger MS gezeigt werden. Allerdings gibt es bislang nur wenige OCT-Analysen von Personen mit progredienter MS, insbesondere keine umfangreichen longitudinalen Untersuchungen. [9]

Um den möglichen Einsatz der OCT als Marker der Neurodegeneration in Personen mit primär progrdienter MS (PwPPMS) zu evaluieren, ist die Untersuchung in der Tiefe von klinisch und bildgebend charakterisierten Kohorten notwendig, die sowohl im Querschnitt, aber auch longitudinal untersucht werden.[10]

Deswegen verfolgte diese Promotionsarbeit drei Ziele: erstens der Aufbau einer solchen progredienten MS-Kohorte, zweitens sollte untersucht werden, ob die OCT geeignet ist, eine mögliche Neurodegeneration der progredienten Multiplen Sklerose in dieser Kohorte zu erfassen und das Ausmaß der retinalen neuroaxonalen Degeneration in Assoziation mit klinischen Parametern zu zeigen. Drittens sollte geprüft werden, ob dieses Analysemodell auch in unterschiedlichen anderen Erkrankungskohorten angewendet werden kann.

4.2 Die Optische Kohärenztomographie und Segmentierung retinaler Schichten

Die OCT ermöglicht eine nicht-invasive Darstellung und Analyse einer retinalen neuroaxonalen Inflammation und Neurodegeneration. Die Retina ist evolutionsgeschichtlich Teil des ZNS und ist in ihrem Aufbau dem Neocortex ähnlich. Damit wird die Retina auch als „Window to the brain“ betitelt und sie eignet sich zur Diagnose, Vorhersage und Verlaufsbeurteilung von inflammatorischen, aber auch neurodegenerativen Prozessen bei unterschiedlichen ZNS-Erkrankungen.

Dafür hat sich die Spectral-Domain optische Kohärenztomographie (SD-OCT) etabliert.[11] Die SD-OCT ist eine nicht invasive *in-vivo* Bildgebung des Augenhintergrundes, bei dem Licht von geringer Kohärenzlänge zur Erstellung von Querschnitts- und 3D-Bildern der Retina mit hoher axialer Auflösung bei hoher Messgeschwindigkeit verwendet wird. [12] Die SD-OCT erlaubt gegenüber der älteren Time-Domain OCT (TD-OCT) eine präzisere und schnellere morphologische Darstellung aller retinaler Schichten um die Sehnervpapille und der perifovealen Makula.[13] Mit einer Geräte-eigenen Segmentierungssoftware können halbautomatisch alle retinalen Schichten segmentiert und volumetrisch erfasst werden.

Relevante Parameter sind dabei die peripapilläre Nervenfaserschicht-Dicke (pRNFL), die als Maß der peripapillären axonalen Schicht in µm misst, das totale Makulavolumen (TMV) und beispielsweise die kombinierte Schicht aus Ganglienzellschicht und innere plexiforme Zellschicht (GCIPL). Die Ergebnisse der Segmentierung und der Analyse werden entsprechend international abgestimmter Kriterien (APOSTEL-Kriterien) berichtet.[14] Dabei wurde in unterschiedlichen Fragestellungen gezeigt, dass insbesondere Veränderungen der globalen pRNFL, aber auch die GCIPL, geeignete Marker für eine retinale neuroaxonale Degeneration sind. [15, 16] Die innere Körnerzellschicht (INL) hingegen wird als Marker für Krankheitsaktivität diskutiert, da gezeigt werden konnte, dass es im Rahmen von entzündlicher Aktivität im ZNS zu einer Verdickung und Schwellung der INL kommen kann. [17] Damit könnte sich die INL als Monitoringparameter therapeutischer Effekte eignen. Passend dazu konnte in einer Kohorte gezeigt werden, dass nur Personen mit stabilen Erkrankungsverlauf nach Therapiebeginn (no evidence of disease activity, NEDA) auch eine Normalisierung der INL unter Immuntherapie zeigten. [17, 18]

4.3 Die Multiple Sklerose

Die Multiple Sklerose ist eine der häufigsten neurologischen Erkrankungen bei jungen Erwachsenen, mit hoher Prävalenz in Nordamerika und Europa. Es handelt sich um eine immunvermittelte chronisch-entzündliche Erkrankung des zentralen Nervensystems, die allein in Deutschland zwischen 200.000-250.000 Menschen betrifft.[19, 20]

Die Prävalenz in Europa, sowie Nordamerika liegt bei über 100 Erkrankten pro 100.000 Einwohner.[21] Weltweit geht man von über 2 Millionen Betroffenen aus.[22] Der Häufigkeitsgipfel der MS liegt im 30. Lebensjahr. Frauen erkranken dabei häufiger als Männer, das Verhältnis variiert je nach Quelle von 2-3:1. [22, 23]

Die Ätiologie der MS ist nicht vollständig verstanden, auslösende genetische Faktoren und Umweltfaktoren werden jedoch diskutiert. Die Theorie einer Autoimmunpathogenese wird im Allgemeinen angenommen und wurde in verschiedenen Studien beschrieben. [24, 25] Dies wird weiter unterstützt durch die Beteiligung von Genen, die in die Immunregulation eingebunden sind und als Risikogene für die Entwicklung einer MS gelten. Auch der Stellenwert in der Immunpathogenese von Umweltfaktoren wie z.B. Vitamin D, Diät oder Rauchen und

virale Erkrankungen wie die infektiöse Mononukleose, ausgelöst durch das Epstein-Barr Virus, ist unstrittig.[22, 26, 27] Ebenso zeigt sich die Ethnie als Einflussfaktor. [21]

Die MS ist dabei charakterisiert durch eine T-, aber auch B-Zell vermittelte chronisch-entzündliche ZNS-Erkrankung, mit Demyelinisierung und neurodegenerative Prozesse.[25, 28]

Ungefähr 85% aller Erkrankten weisen zunächst einen schubförmig-remittierenden Verlauf (RRMS) auf.[29] Die Behinderungsprogression kann durch zwei Mechanismen entstehen. Man unterscheidet zwischen der schubassoziierten Verschlechterung (relapse associated worsening: RAW) und der Verschlechterung unabhängig der Krankheitsaktivität (progression independent of disease activity: PIRA). [30] Während die PIRA früh im Krankheitsverlauf eintritt, bei allen Subtypen auftritt und vor allem im progressiven Stadium die Behinderungsprogression vorantreibt, ist der Mechanismus der RAW eine Verschlechterung durch Schubaktivität. [30]

Ein Schub wird definiert durch eine Dauer der Symptome von mindestens 24 Stunden und mindestens 30 Tage seit dem letzten Schub, sowie dass das Auftreten der neurologischen Symptome nicht durch andere Faktoren (wie z.B. Fieber) begründet ist. [31] Gewöhnlich äußert sich ein Schub durch Symptome wie fokale supratentorielle oder zerebelläre Syndrome, sowie Hirnstammsyndrome oder einer inkompletten Myelitis. Eine häufige Schubmanifestation ist die Optikusneuritis.[31] Die Diagnose eines Erkrankungsschubes ist jedoch nicht trivial und die Abgrenzung eines Erkrankungsschubes von einem „Pseudoschub“, sowie von einer schubunabhängigen Progression, ist im klinischen Alltag eine Herausforderung. Deswegen wird neben der klinischen Beurteilung auch apparative Diagnostik eingesetzt um strukturelle, aber auch funktionelle Defizite zu erfassen.

Die OCT eignet sich nur bedingt zur Diagnosestellung einer Optikusneuritis in der Akutphase, da zumindest MS-assoziierte Optikusneuritiden nur selten mit einer Papillenschwellung einhergehen. [9] Allerdings eignet sich das OCT besonders zum Nachweis der retinalen neuroaxonalen Degeneration nach abgelaufener Optikusneuritis und auch zum Nachweis von Veränderungen unabhängig von Schüben. Diese retinalen Veränderung haben sich als Marker der Neurodegeneration in der Verlaufsbeurteilung von Patienten mit MS etabliert.[32]

Diese retinale Veränderung ist bei der MS insbesondere hilfreich, da unterschiedliche MS-Subtypen mit heterogenem klinischen Verlauf bestehen. [28] Eine schubförmige MS kann in

eine sekundär-progrediente MS (SPMS) übergehen. Der Übergang erfolgt - basierend auf Kohortenbeobachtungen - meistens nach 15 bis 20 Erkrankungsjahren.[33] Die Übergangszeit nennt man auch Transitionsphase, in der Aspekte von RRMS aber auch SPMS auftreten können.[34] Die SPMS kann sich später dann mit oder ohne aufgesetzte Schübe präsentieren (aktive vs. inaktive SPMS). [35]

Bei 5-15% der Erkrankten zeigt sich von Anfang an ein primär-progredienter Verlauf (PPMS).[29] Ungewöhnlich ist hier also der Beginn ohne initiales Schubereignis. Obwohl eine PPMS von einer schleichenden Verschlechterung der neurologischen Defizite geprägt ist, können auch einzelne überlagerte Schübe auftreten.[31] PatientInnen mit PPMS sind zum Zeitpunkt der Erkrankung älter als die restlichen MS-Subtypen und sind häufiger männlich.[36]

Es wird diskutiert, ob es sich bei den verschiedenen Subtypen um eine einzige Krankheitsentität handelt, oder ob es grundsätzlich unterschiedliche Krankheiten innerhalb eines Spektrums sind.[37]

Diagnostiziert wird die MS anhand der derzeitig gültigen McDonald 2017 Kriterien.[38] Diese beruhen auf dem Prinzip der klinischen und paraklinischen zeitlichen und räumlichen Dissemination. Dabei sind neben dem klinischen Verlauf, die Kernspintomographie (MRT) und Liquordiagnostik wichtige diagnostische Parameter. [39] Der Nachweis einer zeitlichen und räumlichen Dissemination ist notwendig zur Abgrenzung monosymptomatischer und -phasischer Erkrankungen und ist damit Teil der Diagnosestellung.[40] Wenn eine Erstmanifestation sich mit einer klinisch und paraklinisch räumlichen Dissemination präsentiert, allerdings die Kriterien der zeitlichen Dissemination nicht erfüllt sind, spricht man von einem klinisch-isolierten Syndrom (KIS).[31, 41, 42] Ein radiologisch-isoliertes Syndrom (RIS) kann hingegen diagnostiziert werden, wenn nach den aktuellen RIS-Kriterien nach Lebrun-Frenay (2023) kernspintomographisch zwar entzündliche Läsionen mit räumlicher Dissemination nachweisbar sind und liquordiagnostisch der Nachweis eines entzündlichen Liquorsyndroms gelingt, allerdings klinisch weder Schübe, noch eine Progression in der Vorgeschichte bestanden haben.[31, 43]

Dem klinischen Monitoring des Erkrankungsverlaufes kommt eine besondere Rolle zu. Die Zunahme der Behinderungsprogression wird mittels des Expanded Disability Status Scale (EDSS) erfasst.[30] Dieser umfasst unterschiedliche Funktionsscores (FS), die zur Beurteilung

des EDSS beitragen. Eine besondere Rolle zur EDSS-Berechnung kommt der Gehfähigkeit, aber auch anderen Funktionsscores wie dem zerebellären FS, dem sensorischen FS, den vegetativen FS und beispielsweise dem cerebralen FS (u.a. Kognition) zu. [29]

Therapeutisches Ziel ist einerseits die Reduktion von Erkrankungsschüben und andererseits ein Verlangsamen oder Aufhalten der Behinderungsprogression. Man spricht dabei auch von einer „disease modifying therapy (DMT)“, da eine MS-spezifische Therapie den MS-Erkrankungsverlauf beeinflussen, allerdings nicht heilen kann.[31, 37] Die verwendeten Substanzen wirken über unterschiedliche Mechanismen, von Immunmodulation und Immunsuppression bis hin zur Immunrekonstitution.[31] Die Substanzen werden entsprechend ihrer Zulassungsstudien in Wirksamkeitskategorien von 1 bis 3 eingeteilt. [31] Dabei gibt es Medikamente die isoliert oder in Kombination B-, T-Zell oder Zytokin-basierte Pathways reversibel oder irreversibel adressieren.

4.4 Die Optische Kohärenztomographie in der Multiplen Sklerose

Für die schubförmige MS konnte konsistent gezeigt werden, dass mittels OCT sowohl ein Monitoring der Inflammation, aber auch eine Beurteilung der Neurodegeneration möglich ist. [15, 44, 45] Allerdings sind Daten zur progredienten MS weitaus spärlicher und insbesondere longitudinale OCT-Daten liegen bei dieser Form der MS nur vereinzelt vor. [46] Deswegen besteht insbesondere für Personen mit PPMS (PwPPMS) der Bedarf an weiteren Untersuchungen, insbesondere auch der Korrelation retinaler Bildgebungsdaten mit klinischen Outcome-Parametern.[47] Auch könnte sich die OCT zunehmend für das nicht-invasive Monitoring von therapeutischen Effekten und neurodegenerativen Erkrankungsverläufen etablieren. [10]

Neben dem Monitoring ist auch eine Rolle des OCT in der Diagnostik der MS vorstellbar. Noch spielt die OCT zwar keine Rolle in den etablierten Diagnosekriterien der MS.[39] Allerdings hat die Magnetic Resonance Imaging In Multiple Sclerosis – Gruppe (MAGNIMS Gruppe) vorgeschlagen, die Optikusneuritis als 5. Raum zum Nachweis der räumlichen Dissemination zuzulassen. [48] Damit könnte eine Zwischenaugendifferenz (intereye difference) als Nachweis einer früheren Optikusneurits entsprechend einer Läsion im N. opticus gewertet werden. [49, 50]

Eine OCT-Routineuntersuchung aller Erstmanifestationen einer Multiplen Sklerose wäre dann wünschenswert.[1] Da 50% aller diagnostizierter Optikusneuritiden (ON) auf eine MS zurückzuführen sind, zeigt sich die hohe Relevanz der OCT im Rahmen dieser Erkrankung. [51]

4.5 Die Optische Kohärenztomographie in anderen Indikationen am Beispiel der Phenylalaninhydroxylase-Defizienz

Die Anwendung der OCT ist potenziell auch für andere Erkrankungen interessant, die mit zerebraler Neurodegeneration einhergehen können.[52-56]

Die klassische Phenylketonurie (PKU) ist eine autosomal-rezessiv vererbte Stoffwechselerkrankung, bei der es zu einem behandlungsbedürftigen Mangel des Enzyms Phenylalaninhydroxylase (PAH) kommt, wodurch der Abbau der Aminosäure Phenylalanin gestört ist und diese vermehrt im Körper anfällt.[57] Bei einem nicht-behandlungsbedürftigen Mangel an PAH spricht man von einer Phenylalaninhydroxylase-Defizienz (PAH-Defizienz).[58] Die Prävalenz variiert weltweit stark und ist abhängig von Region und Ethnie, liegt jedoch bei ungefähr 1:10.000 Neugeborenen. [59]

Die Phänotypen reichen von milder Ausprägung mit gering erhöhter Phenylalaninkonzentration, bis hin zu schwerer Ausprägung mit deutlich erhöhter Phenylalaninkonzentration. Die Symptome variieren damit auch zwischen weniger ausgeprägten Krankheitsverläufen mit unauffälligem Erscheinungsbild bis hin zu stark ausgeprägten Verläufen mit neuropsychologischen Komplikationen wie geistiger Retardierung, Krampfanfällen und Spastiken.[60] Weitere allgemeine Erkrankungssymptome können Übelkeit, Ekzeme oder unangenehmer Körpergeruch sein.[58] Um schwere Krankheitsverläufe vorzubeugen, ist die PKU mittlerweile weit verbreitet Teil des Neugeborenenscreenings.[61] Wie oben bereits beschrieben, muss bei der Phenylalaninhydroxylase-Defizienz generell, anhand der alterstypischen Grenzwerte, zwischen einer therapiebedürftigen und nicht-therapiebedürftigen Defizienz unterschieden werden.

Therapeutisch ist es wichtig, die Phenylalaninkonzentration zu senken. Therapieoption ist zum einen, eine strikte Diät mit Verzicht auf Phenylalanin in Mahlzeiten, da die hohe Konzentration von anfallendem Phenylalanin Hauptfaktor für Dysfunktion des ZNS ist. [59] Zum anderen kann

eine pharmakologische Therapie mit Tetrahydrobiopterin (BH_4) bei einigen PatientInnen Wirkung zeigen und kann als „Chaperon-Therapie“ die Toleranz für Phenylalanin erhöhen.[59, 62] Unter den therapiebedürftigen Verläufen kann dann in BH_4 -responsive und BH_4 non-responsive Hyperphenylanämie eingeteilt werden.[61] Bei allen PatientInnen, die eine BH_4 Responsivität aufweisen, ist eine Chaperon-Therapie zugelassen. Entscheidend für die Therapieziele sind schlussendlich die Phenylalaninkonzentrationen mit altersabhängigen Grenzwerten. [57]

In der Diagnostik ist die Erhebung der Phenylalanin-Konzentration eine sehr gute Möglichkeit zur Beurteilung der Effizienz der gewählten Therapie, generell ist es jedoch eine Herausforderung, optimale Behandlungsziele festzulegen. [58, 63] Einheitlich ist lediglich eine Therapienotwendigkeit ab Phenylalanin-Konzentrationen von über 600μmol/L und das unter Konzentrationen von 360 μmol/L keine Notwendigkeit besteht. [58] Diskutabel ist also u.a. die Therapieindikation für die Zwischenwerte und anhand welchen Markers man diese stellen kann.

Es besteht Evidenz, dass die PAH-Defizienz zu neuroaxonaler Degeneration führt.[64] Vor allem sind Läsionen der weißen Substanz als Marker für die Progression der PKU bekannt. [65] Diese Läsionen treten abhängig von Alter und metabolischer Einstellung der PatientInnen auf.[66, 67]

Um die offenen Fragen zu adressieren, kann also die Untersuchung der Korrelation zwischen Therapieeinstellung und Ausmaß der Neurodegeneration dienen, um eine entscheidende Einschätzung der Effizienz der Therapie zu ermöglichen. Ein Biomarker für diese Neurodegeneration wäre ein bedeutsames Instrument in der Behandlung der PAH-Defizienz – in der Indikationsstellung, bei Bestimmung von Therapiezielen sowie der Beurteilung dieser Therapie.

Die SD-OCT könnte als nicht-invasive, sensible und benutzer-unabhängige Untersuchungsmöglichkeit der Retina zur Einschätzung der neuroaxonalen Degeneration bei PAH-Defizienz-PatientInnen dienen und somit Rückschluss auf den Effekt der Therapie erlauben. In Studien zu metabolisch bedingter Neurodegeneration zeigt die OCT klare Vorteile

in der Diagnostik, daher gilt sie auch bei der PKU als vielversprechendes diagnostisches Instrument.[68, 69]

4.6 Ergebnisse

Beide Veröffentlichungen bieten gute Einblicke in die Möglichkeiten der OCT als submodernen Marker für Neurodegeneration.
Um die Fragestellung der Erfassung von Neurodegeneration und Neuroinflammation zu beantworten, wurde eine große Kohorte von Personen mit MS zusammengeführt und gemeinsam analysiert. Insgesamt wurden 57 PPMS-PatientInnen, 62 RRMS-PatientInnen und 61 Gesundkontrollen untersucht. 83 Augen wurden an der MSK am CIRRUS Gerät untersucht, sowie 260 Augen an der LMU, mit einem SPECTRALIS Gerät, eingeschlossen worden. Alle Gesundkontrollen wurden an der LMU aufgenommen. Das Durchschnittsalter bei der Baseline OCT-Untersuchung der PPMS-Kohorte beträgt 54 Jahre, das der RRMS-Kohorte 37 Jahre und das der Gesundkontrollen 36 Jahre. Der initiale EDSS der PPMS-PatientInnen lag mit 4.25 höher als bei den RRMS-PatientInnen mit 2. Im Median wurde die PPMS-Kohorte über 40 Monate beobachtet und die RRMS-Kohorte über 28 Monate. Das Hauptergebnis dieser Veröffentlichung ist die Korrelation zwischen der Verschlechterung der Gehfähigkeit und der retinalen Degeneration im OCT von PPMS-PatientInnen. Damit wird die Hypothese gestärkt, dass die OCT als Verlaufsmarker der MS dienen kann.

Hervorzuheben ist, dass anhand von t-Test und einer ANCOVA-Analyse bei der jährlichen relativen Veränderung der TMV, der GCIPL, sowie der ONPL bei PPMS-PatientInnen mit instabiler Gehfähigkeit ein Effekt festgestellt wird. Dabei zeigt sich ein signifikanter Unterschied (*p=0.*002) an Nervenfaserschichtdicke der TMV, GCIPL und ONPL, zwischen PPMS-PatientInnen mit stabiler Gehstrecke und PPMS-PatientInnen mit verschlechterter Gehstrecke. Es kann kein signifikanter Unterschied zwischen RRMS und PPMS festgestellt werden.

In der Kohorte kann bestätigt werden, dass die jährliche relative Verschlechterung der pRNFL bei PatientInnen mit MS (Mean in %= -0.730; *p= 0.002*) größer ist als die von gesunden Probanden (Mean in %= -0.131; *p=0.002*). Es kann wiederum kein signifikanter Unterschied zwischen PPMS und RRMS in dieser Kohorte gezeigt werden. Damit sind unsere Ergebnisse vereinbar mit bereits bestehenden Analysen.[8]

In der Veröffentlichung zur OCT bei PAH-Defizienz ist eines der Hauptergebnisse die Feststellung, dass spät diagnostizierte PatientInnen, die eine Therapie benötigen, eine fortgeschrittene retinale Degeneration aufweisen.

Des Weiteren zeigen PKU-PatientInnen, die früh diagnostiziert und diätetisch eingestellt waren (ETPKU), unterschiedlich ausgeprägte neuroaxonale Degeneration, abhängig von Alter und metabolischer Einstellung. Interessanterweise zeigt sich vor allem bei über 18-jährigen PKU-PatientInnen, die eine Therapie benötigen und nicht BH_4 -responsive sind, eine signifikante Verringerung der GCIPL (Mean= 0.58mm^3; SD= 0.03; *p=0.021*) als auch der IRL (Mean= 1.59mm^3; SD= 0.07; *p= 0.033*). ETPKU-PatientInnen, zeigten eine Verringerung der GCIPL im Vergleich zu der Gesundkontrolle (Mean ± SD 0.59 ±0.04 vs. 0.61 ± 0.05mm^3, *p = 0.035*). Eine Analyse der pädiatrischen ETPKU-PatientInnen zeigt keine signifikanten Unterschiede der makulären Schichten zu denen der Gesundkontrollen, wenn jedoch eine Analyse anhand der Phenylalanin-Konzentrationen gemacht wird, kann eine Verringerung der pRNFL und GCIPL-Dicke im Vergleich zur Gesundkontrolle festgestellt werden.

5. Zusammenfassung

Im klinischen Alltag besteht ein großer Bedarf zum Monitoring neuroinflammatorischer und neurodegenerativer Erkrankungen. Eine solche Methodik soll idealerweise nicht nur valide, reliabel, Kosten-effektiv und nicht-invasiv, sondern auch reproduzierbar, nachvollziehbar und unabhängig vom Benutzer sein.

Deswegen verfolgte diese Promotionsarbeit drei Ziele: erstens der Aufbau einer solchen progredienten MS-Kohorte, zweitens sollte untersucht werden, ob die OCT geeignet ist eine mögliche Neurodegeneration der progredienten Multiplen Sklerose zu erfassen und das Ausmaß der retinalen neuroaxonalen Degeneration in Assoziation mit klinischen Parametern zu zeigen. Drittens sollte geprüft werden, ob dieses Analysemodell auch in unterschiedlichen anderen Erkrankungskohorten angewendet werden kann.

Die Multiple Sklerose (MS) ist eine häufige neurologische Erkrankung bei jungen Erwachsenen. Sie ist immunvermittelt und betrifft weltweit über 2 Millionen Menschen, wobei Frauen

häufiger betroffen sind als Männer. Die Krankheit ist durch Entzündungsherde im zentralen Nervensystem gekennzeichnet, die zu Myelinschädigung und neuroaxonaler Degeneration führen. Die Diagnose erfolgt anhand von Kernspintomographie und Liquordiagnostik nach den McDonald-Kriterien. Die Symptome sind vielfältig und können schubweise oder progressiv auftreten. Etwa 85% der Patienten haben einen schubförmig-remittierenden Verlauf, während einige in eine sekundär progrediente Phase übergehen. Eine kleine Anzahl von Patienten hat einen primär progressiven Verlauf (5-10%). Auch aufgrund der geringeren Inzidenz der PPMS, gibt es weniger Studiendaten zu diesem Phänotyp. Zur Bewertung der Gehfähigkeit verwenden wir den Ambulation Score in unserer Studie, der auch den EDSS beeinflusst.

Als weitere Kohorte wurde eine bestehende Kohorte mit angeborener Stoffwechselerkrankung ausgewählt. Die PKU ist eine erbliche Stoffwechselerkrankung, die durch einen Mangel an Phenylalaninhydroxylase verursacht wird, was eine PAH-Defizienz bedeutet und zu einem Anstieg von Phenylalanin im Körper führt. Eine PAH-Defizienz kann zu neuroaxonaler Degeneration führen, wobei Läsionen der weißen Substanz als Marker für die Krankheitsprogression gelten. Die Untersuchung der Korrelation zwischen Therapie und Neurodegeneration könnte die Effizienz der Behandlung besser einschätzen lassen. Die SD-OCT, könnte als diagnostisches Instrument zur Beurteilung der neuroaxonalen Degeneration bei PKU-Patienten dienen und so Rückschlüsse auf den Therapieerfolg ermöglichen.

Im Ergebnis konnten alle 3 Ziele der Promotionsarbeit erreicht werden:

Nach Zusammenstellung einer großen progredienten MS-Kohorte konnte gezeigt werden, dass die OCT geeignet ist eine mögliche Neurodegeneration der progredienten Multiplen Sklerose zu erfassen. Auch das Ausmaß der retinalen neuroaxonalen Degeneration in Assoziation mit klinischen Parametern konnte gezeigt werden, indem eine Korrelation zwischen Gehfähigkeit und retinaler Degeneration bei PPMS-PatientInnen dargestellt wurde. Bei PPMS-PatientInnen mit instabiler Gehfähigkeit wird ein signifikanter Unterschied in der Nervenfaserschichtdicke im Vergleich zu denen mit stabiler Gehfähigkeit festgestellt. Es gibt in unserer Kohorte keinen signifikanten Unterschied zwischen RRMS und PPMS in Bezug auf die jährliche relative Verschlechterung der pRNFL. Drittens haben wir das Analysemodell auch auf eine andere Kohorte übertragen und zeigen, dass spät diagnostizierte PatientInnen eine fortgeschrittene retinale Degeneration aufweisen. Früh diagnostizierte und diätetisch behandelte PatientInnen zeigten unterschiedliche Grade an neuroaxonalen Schädigung, abhängig von Alter und

metabolischer Einstellung. Besonders bei über 18-jährigen PKU-PatientInnen, die nicht auf BH_4 ansprechen, wird eine signifikante Verringerung der GCIPL und IRL beobachtet.
Auch in einer dritten Veröffentlichung (Mulazzani et al.), die nicht in diese Promotionsarbeit einfloß, konnten wir die OCT als Analysemodell nutzen.

5.1 Beitrag zu Paper I: Inner Retinal Layer Changes Reflect Changes in Ambulation Score in Patients with Primary Progressive Multiple Sclerosis

Die Rekrutierung der PatientInnen erfolgte durch mich zum einen in der Neuroimmunologischen Ambulanz des Klinikum Großhaderns (KUM), zum anderen in der Marianne-Strauss-Klinik (MSK) in Berg am Starnberger See. Die Daten wurden durch mich anonymisiert zu einer Kohorte, im Sinne einer Datenbank, zusammengeführt.
An beiden Zentren werden seit Jahren OCT-Untersuchungen in der klinischen Routine eingesetzt (MSK OCT: CIRRUS SD, Zeiss; KUM OCT: SPECTRALIS SD, Heidelberg Engineering). Zusätzlich erfolgte durch mich der Einschluss einer gesunden Kontrollkohorte sowie einer RRMS-Vergleichskohorte. Die gesunden Kontrollen wurden sowohl aus der OCT-Datenbank der KUM extrahiert als auch durch mich neu rekrutiert und für neue OCT-Kontrolluntersuchungen einbestellt.
Ich war verantwortlich für die Organisation der Vorstellungstermine, die Studienaufklärung, sowie die Einholung der Einverständniserklärung der PatientInnen. Des Weiteren führte ich die visuelle Anamnese und Funktionsprüfung, als auch die OCT-Untersuchungen der prospektiven Datenerhebung durch. Die Qualitätskontrolle und Segmentierung dieser Bilder oblagen mir, ebenso die Datenbankpflege. Ich war an der statistischen Analyse und am originalen Manuskript beteiligt, sowie schlussendlich am Manuskript-Editing.
Die Datenanalyse erfolgte in Zusammenarbeit mit Stefan Buchka, Institute of Medical Information Processing, Biometry, and Epidemiology, Faculty of Medicine Munich, und zusammen mit Jonathan Gernert.
Die geteilte Erstautorenschaft ergab sich aus der engen Zusammenarbeit zwischen Herrn Gernert und mir während des Schreibprozesses. Durch diese Zusammenarbeit konnte ich mein Wissen im Verfassen von Aufsätzen und wissenschaftlichen Artikeln erweitern. Ich war intensiv in den Überarbeitungs- und Korrekturprozess eingebunden und habe es sehr genossen, mein Projekt am Ende zu visualisieren.

5.2 Beitrag zu Paper II: Optical Coherence Tomography to Assess Neurodegeneration in Phenylalanine Hydroxylase Deficiency

Im Rahmen der Promotionsarbeit habe ich in Zusammenarbeit mit Fr. PD Dr. A. Lotz-Havla das neurovisuelle System einer Kohorte mit PHD in unserem NeuroVisionLab bezüglich struktureller und funktioneller Defizite untersucht. Das Paper wurde in Zusammenarbeit des Haunerschen Kinderklinikums München und dem Institut für klinische Neuroimmunologie des LMU-Klinikums Großhadern veröffentlicht. Als Promotionsstudentin in der Ambulanz für Neuroimmunologie und Teil des NeuroVisionLabs unter Leitung von PD Dr. med. Joachim Havla, war ich für die Organisation der Vorstellungstermine der prospektiven Untersuchungen, die Studienaufklärung, sowie die Einholung der Einverständniserklärung der PatientInnen zuständig. Des Weiteren führte ich selbstständig die visuelle Anamnese und Funktionsprüfung, als auch die OCT-Untersuchungen, im Sinne einer prospektiven Datenasservation, durch. Die Qualitätskontrolle und Segmentierung dieser Bilder oblagen mir, ebenso die Datenbankpflege, aus welcher ich retrospektiv Daten für unsere Gesundkontrollen zog. Die Analyse habe ich begleitet und war am Manuskript-Editing beteiligt.

6. Abstract (English)

In clinical practice, there is a significant need for monitoring neuroinflammatory and neurodegenerative diseases. Ideally, such a method should be cost-effective, non-invasive, reproducible, transparent, and user independent. Part of our research goal was to determine whether SD-OCT can serve as such a method in clinical practice. Many studies have already investigated the relationship between disability progression in MS and OCT imaging, and significant potential is seen in this imaging technique.

MS is a common neurological disease in young adults. It is immune-mediated and affects over 2 million people worldwide, with women being more frequently affected than men. The disease is characterized by inflammatory lesions in the central nervous system, leading to myelin damage and neuroaxonal degeneration. Diagnosis is based on MRI and cerebrospinal fluid analysis according to the McDonald criteria. Symptoms vary and can occur in relapsing-remitting or progressive forms. About 85% of patients have a relapsing-remitting course, while

some transition to a secondary progressive phase. A small number of patients have a primary progressive course (5-10%). Due to the lower incidence of PPMS, there are fewer study data on this phenotype. In our study, we use the Ambulation Score to assess walking ability, which also influences the EDSS.

Another cohort selected was an existing cohort with a congenital metabolic disorder. PKU (phenylketonuria) is an inherited metabolic disorder caused by a deficiency of phenylalanine hydroxylase (PAH), leading to an increase of phenylalanine in the body. A PAH deficiency can result in neuroaxonal degeneration, with white matter lesions as considered markers of disease progression. Investigating the correlation between therapy and neurodegeneration could better assess the efficiency of treatment. SD-OCT could serve as a diagnostic tool for evaluating neuroaxonal degeneration in PKU patients, thereby providing insights into the success of the therapy.

The results of the study achieved all three objectives of the dissertation: After assembling a large cohort of progressive MS patients, it was demonstrated that OCT is suitable for detecting potential neurodegeneration in progressive multiple sclerosis. The extent of retinal neuroaxonal degeneration in association with clinical parameters was also shown by illustrating a correlation between walking ability and retinal degeneration in PPMS patients. A significant difference in nerve fiber layer thickness was observed in PPMS patients with unstable walking ability compared to those with stable walking ability. There is no significant difference between RRMS and PPMS in our cohort regarding the annual relative deterioration of the pRNFL. Thirdly, we applied the analysis model to another cohort and demonstrated that late-diagnosed patients exhibit advanced retinal degeneration. Early diagnosed and diet-treated patients showed varying degrees of neuroaxonal damage, depending on age and metabolic control. A significant reduction in GCIPL and IRL is particularly observed in PKU patients over 18 years old who do not respond to BH_4.

In a third publication (Mulazzani et al.), which was not included in this dissertation, we were also able to use OCT as an analysis model.

6.1 Contribution to Paper I: Inner Retinal Layer Changes Reflect Changes in Ambulation Score in Patients with Primary Progressive Multiple Sclerosis

The recruitment of patients was carried out by me, on the one hand, at the Neuroimmunology Outpatient Clinic of Klinikum Großhadern (KUM), and on the other hand, at the Marianne-Strauß-Klinik (MSK) in Berg near Lake Starnberg. Inclusion criteria were the presence of progressive MS (PPMS, SPMS, PMS), the availability of clinical routine data and a baseline OCT examination, as well as at least one follow-up OCT and one clinical follow-up examination with a multivariable clinical test battery. This included various clinical scales such as the EDSS or MSFC, and other clinical tests, such as walking distance, the 25-foot walking test, or the 9-hole peg test (9HPT). These follow-up assessments had to be conducted at least one year after baseline. I anonymized these data and compiled them into a cohort in the form of a database.

At both centers, OCT examinations have been used in clinical routine for years (MSK OCT: CIRRUS SD, Zeiss; KUM OCT: SPECTRALIS SD, Heidelberg Engineering). Additionally, I included a healthy control cohort and a comparison cohort of RRMS patients. The healthy controls were either extracted from the OCT database of KUM or newly recruited by me and invited for new OCT control examinations.

I was responsible for organizing the appointments, providing study information, and obtaining the patients' informed consent. Furthermore, I conducted the visual anamnesis, functional testing, and the OCT examinations as part of prospective data collection. The quality control and segmentation of these images were also under my responsibility, as well as maintaining the database. I was involved in the analysis and in drafting the original manuscript, as well as in the final editing of the manuscript.

The data analysis was carried out in collaboration with Stefan Buchka, Institute of Medical Information Processing, Biometry, and Epidemiology, Faculty of Medicine Munich, and together with Jonathan Gernert.

The shared first authorship arose from the close collaboration between Mr. Gernert and me during the writing process. Through this collaboration, I was able to expand my knowledge of

drafting papers and scientific articles. I was heavily involved in the revision and correction process and thoroughly enjoyed visualizing my project in the end.

6.2 Contribution to Paper II: Optical Coherence Tomography to Assess Neurodegeneration in Phenylalanine Hydroxylase Deficiency

As part of my doctoral thesis, I investigated the neurovisual system of a cohort with PHD in our NeuroVisionLab, regarding structural and functional deficits in collaboration with Dr. A. Lotz-Havla. The paper was published in cooperation with the Hauner Children's Hospital in Munich and the Institute of Clinical Neuroimmunology at the LMU Klinikum Großhadern.

As a doctoral student in the Neuroimmunology Outpatient Clinic and a member of the NeuroVisionLab under the direction of Dr. Joachim Havla, I was responsible for organizing the appointments for prospective investigations, providing study information, and obtaining informed consent from the patients. Furthermore, I independently conducted the visual anamnesis, functional testing, and OCT examinations as part of prospective data collection.

I was in charge of the quality control and segmentation of these images, as well as maintaining the database, from which I retrospectively extracted data for our healthy controls. I contributed to the analysis and was involved in the manuscript editing process.

7. Veröffentlichung I

International Journal of *Molecular Sciences*

MDPI

Article

Inner Retinal Layer Changes Reflect Changes in Ambulation Score in Patients with Primary Progressive Multiple Sclerosis

Jonathan A. Gernert [1,†], Luise Böhm [1,†], Michaela Starck [2], Stefan Buchka [3], Tania Kümpfel [1,4], Ingo Kleiter [2,5,‡] and Joachim Havla [1,4,*,‡]

[1] Institute of Clinical Neuroimmunology, Ludwig-Maximilians-Universität München, 81377 Munich, Germany
[2] Marianne-Strauß-Klinik, Behandlungszentrum Kempfenhausen für Multiple Sklerose Kranke gGmbH, 82335 Berg, Germany
[3] Institute of Medical Information Processing, Biometry, and Epidemiology, Faculty of Medicine, Ludwig-Maximilians-Universität München, 81377 Munich, Germany
[4] Biomedical Center and University Hospital, Ludwig-Maximilians-Universität München, 82152 Planegg-Martinsried, Germany
[5] Department of Neurology, Ruhr-University Bochum, 44791 Bochum, Germany
* Correspondence: joachim.havla@med.uni-muenchen.de
† These authors contributed equally to this work.
‡ These authors contributed equally to this work.

Abstract: The establishment of surrogate markers to detect disability progression in persons with multiple sclerosis (PwMS) is important to improve monitoring of clinical deterioration. Optical coherence tomography (OCT) could be such a tool. However, sufficient longitudinal data of retinal neuroaxonal degeneration as a marker of disease progression exist only for PwMS with a relapsing–remitting course (RRMS) so far. In contrast, longitudinal data of retinal layers in patients with primary-progressive MS (PPMS) are inconsistent, and the association of OCT parameters with ambulatory performance in PwMS has rarely been investigated. We aimed to investigate the relative annual rates of change in retinal layers in PwMS (RRMS and PPMS) compared with healthy controls (HC) using OCT and to evaluate their association with ambulatoryfunctionalscore (AS) worsening in PPMS. A retrospective analysis of a longitudinal OCT dataset of the retinal layers of PwMS and HC from two MS centers in Germany was performed. Walking ability was measured over a standardized distance of 500 m, and changes during the observation period were categorized using the AS and the expanded disability status scale (EDSS). 61 HC with 121 eyes and 119 PwMS (PPMS: 57 patients with 108 eyes; RRMS: 62 patients with 114 eyes) were included. The median follow-up time for PwMS was 3 years. The relative annual change of pRNFL (peripapillary retinal nerve fiber layer) and INL (inner nuclear layer) was significantly different in PwMS compared with HC. RRMS and PPMS subgroups did not differ in the annual atrophy rates. In patients with PPMS, worsening of the AS was significantly associated with increased thinning of the TMV (total macular volume), GCIP (ganglion cell and inner plexiform layer), and ONPL (outer nuclear and outer plexiform layer) (all p-value < 0.05, $r > 0.30$). For every −0.1% decrease in the TMV, GCIP, and ONPL, the risk of a deterioration in the AS increased by 31% (hazard ratio (HR): 1.309), 11% (HR: 1.112), and 16% (HR: 1.161), respectively. In addition, worsening EDSS in PPMS was significantly associated with the relative annual atrophy rates of pRNFL, TMV, and GCIP (all p-value < 0.05). Disability progression in PPMS can be measured using OCT, and increasing annual atrophy rates of the inner retinal layers are associated with worsening ambulation. OCT is a robust and side-effect-free imaging tool, making it suitable for routine monitoring of PwMS.

Keywords: multiple sclerosis (MS); relapsing–remitting multiple sclerosis (RRMS); primary progressive multiple sclerosis (PPMS); optical coherence tomography (OCT); ambulatory functional score

Citation: Gernert, J.A.; Böhm, L.; Starck, M.; Buchka, S.; Kümpfel, T.; Kleiter, I.; Havla, J. Inner Retinal Layer Changes Reflect Changes in Ambulation Score in Patients with Primary Progressive Multiple Sclerosis. *Int. J. Mol. Sci.* **2023**, *24*, 12872. https://doi.org/10.3390/ijms241612872

Academic Editor: Sang Won Suh

Received: 20 July 2023
Revised: 9 August 2023
Accepted: 13 August 2023
Published: 17 August 2023

1. Introduction

Disability progression in PwMS is predominantly documented as a worsening in walking ability (ambulatory functional score, AS) with an increase in EDSS (expanded disability status scale) score. However, the interval walking distance score is highly dependent on daily performance as well as other internal factors [1–3]. Therefore, it is necessary to use alternative, reliable, reproducible, and validated surrogate markers to determine disability progression independent of the deterioration of the AS as part of the EDSS, the current gold standard.

Optical coherence tomography (OCT) could be such a marker: OCT has been used to study retinal imaging markers in persons with multiple sclerosis (PwMS) [4]. However, most analyses were performed in cohorts with relapsing–remitting MS (RRMS), and results about primary-progressive MS (PPMS) are limited and so far inconsistent: No significant changes in retinal layer thicknesses and/or volumes were reported in longitudinal studies for PPMS [5,6]. One study demonstrated that subjects with PPMS show less retinal atrophy compared with patients with other disease courses of MS (RRMS and secondary-progressive MS (SPMS)) [7]. In contrast, increased retinal thinning has been described in PPMS compared with healthy controls (HC), RRMS, and/or SPMS cohorts [8–13]. In addition, retinal layer thickness in PwMS has mostly been studied in relation to the EDSS score, visual acuity, or cognitive function [14–17].

To demonstrate that OCT may be a surrogate marker of disability progression in PPMS, we performed a retrospective cross-sectional and longitudinal cohort analysis of PwMS compared with HC and examined the association with worsening AS in PPMS: First, we compared OCT parameters cross-sectionally. Second, the relative annual change rates of different retinal layers were analyzed between the cohorts. Third, an association between longitudinal OCT parameters and walking ability was evaluated in PPMS.

2. Results

2.1. Study Cohorts

In total, 180 subjects and 343 eyes were included: 61 HC with 121 eyes and 119 PwMS with 222 eyes (PPMS: 57 patients with 108 eyes; RRMS: 62 patients with 114 eyes). The three cohorts (HC, RRMS, and PPMS) differed significantly in terms of gender distribution, age at baseline OCT (OCT_{bas}), number of follow-up OCT examinations included, and follow-up duration in months. PPMS patients were more often male, were older (mean ± standard deviation (SD) in years: 45.1 ± 10.1), had a higher EDSS score at OCT_{bas} (median: 4.3), and had a longer disease duration (initial manifestation to OCT_{bas}) (median: 7 years) than the RRMS cohort (age: 30.5 ± 10.5; $p < 0.001$; EDSS score: 2.0; $p < 0.001$; disease duration: 2 years; $p < 0.002$). The median overall follow-up time for PwMS was 3 years (interquartile range (IQR): 2–5). Demographic and clinical data are reported in Table 1.

2.2. Cross-Sectional Retinal Layer Analysis

In a gender- and age-adjusted mixed linear model, PwMS showed a significantly reduced pRNFL thickness compared with HC at OCT_{bas} (mean in µm: 94.5 vs. 100.2; $p = 0.002$). Additionally, the TMV and GCIP volumes were significantly decreased in PwMS in comparison to HC (both $p < 0.001$). When comparing RRMS and PPMS patients in terms of retinal layers at OCT_{bas}, no significant differences were found after adjustment for *gender*, *age at* OCT_{bas}, and *disease duration*. However, the mean absolute pRNFL thickness was higher in PPMS than in RRMS, with a subthreshold effect (mean in µm: 96.5 vs. 91.5; $p = 0.072$). The cross-sectional retinal layer analysis at OCT_{bas} is reported in Table 2.

Table 1. Demographic and clinical data.

	HC	PPMS	RRMS	*p*-Value HC vs. PPMS	*p*-Value HC vs. RRMS	*p*-Value PPMS vs. RRMS
General Demographic Data						
Total subjects (*n*)	61	57	62			
Total eyes (*n*)	121	108	114			
Eyes scanned at Cirrus (*n*)	0	44	39			
Eyes scanned at Spectralis (*n*)	121	64	75			
Female, *n* (% of subjects)	38 (62%)	25 (44%)	40 (65%)	***0.045*** [1]	*0.798* [1]	***0.024*** [1]
Age at OCT_{bas}, mean ± SD (years)	36.64 ± 12.82	54.12 ± 10.68	37.19 ± 10.75	***<0.001*** [2]	*0.796* [2]	***<0.001*** [2]
Number of OCT scans, median (range: minimum to maximum)	2 (2–5)	3 (2–7)	3 (2–7)	***<0.001*** [3]	***<0.001*** [3]	*0.377* [3]
Follow-up time, median (IQR) (months)	7 (6–21)	40 (22–76.2)	28 (18.75–64.5)	***<0.001*** [3]	***<0.001*** [3]	*0.060* [3]
Multiple-Sclerosis-Specific Data						
Age at initial onset, mean ± SD (years)		45.09 ± 10.10	30.52 ± 10.53			***<0.001*** [2]
Disease duration, median (IQR) (years)		7 (4–10.5)	2 (0–10)			***0.002*** [3]
Immunotherapy during observation period, *n* (treated subjects)/N (information available) (% of N)		34/44 (77%)	53/59 (90%)			*0.082* [1]
EDSS at OCT_{bas}, median (IQR)		4.25 (3.00–6.00)	2.0 (1.75–3.50)			***<0.001*** [2]
Deterioration in ambulatory functional score (AS), *n* (deteriorated subjects)/N (information available) (% of N)		16/37 (43%)	9/50 (18%)			***0.010*** [1]

In total, 180 subjects and 343 eyes were included. Comparison of demographic and multiple-sclerosis-specific data are shown at baseline optical coherence tomography (OCT_{bas}). Significance was set at $p < 0.05$. EDSS: expanded disability status scale; HC: healthy controls; IQR: interquartile range; *n*: number; OCT: optical coherence tomography; PPMS: primary-progressive multiple sclerosis; RRMS: relapsing–remitting multiple sclerosis; SD: standard deviation. [1] Chi-squared test. [2] *t*-Test. [3] Kruskal–Wallis test.

Table 2. Cross-sectional retinal layer analysis at baseline OCT.

	HC vs. PwMS				PPMS vs. RRMS			
	HC	**PwMS**	**ß (SE)**	***p*-Value** [1]	**PPMS**	**RRMS**	**ß (SE)**	***p*-Value** [2]
Peripapillary Scan (MSK and LMU)								
pRNFL, mean in µm (95% CI) N (eyes)	**100.24 (97.36–103.12)** 121	**94.47 (92.43–96.52)** 222	***−5.765 (1.82)***	***0.002***	96.54 (92.99–100.10) 108	91.45 (87.99–94.91) 114	*5.091 (2.81)*	*0.072*
Macula Scan (LMU)								
TMV, mean in mm^3 (95% CI) N (eyes)	**8.85 (8.76–8.94)** 118	**8.62 (8.54–8.71)** 138	***−0.221 (0.06)***	***<0.001***	8.66 (8.54–8.79) 63	8.55 (8.43–8.66) 75	*0.115 (0.10)*	*0.232*
GCIP, mean in mm^3 (95% CI) N (eyes)	**1.14 (1.11–1.16)** 118	**1.05 (1.02–1.07)** 138	***−0.093 (0.01)***	***<0.001***	1.05 (1.02–1.09) 63	1.02 (0.99–1.06) 75	*0.033 (0.03)*	*0.266*
INL, mean in mm^3 (95% CI) N (eyes)	0.97 (0.95–0.98) 118	0.98 (0.96–0.99) 138	*0.008 (0.01)*	*0.434*	0.97 (0.95–1.00) 63	0.97 (0.95–0.99) 75	*0.003 (0.02)*	*0.850*
ONPL, mean in mm^3 (95% CI) N (eyes)	2.593 (2.529–2.657) 120	2.614 (2.555–2.674) 130	*0.022 (0.05)*	*0.630*	2.632 (2.563–2.700) 63	2.571 (2.505–2.638) 67	*0.060 (0.05)*	*0.269*

Retinal layer thickness and volumes at baseline OCT (OCT_{bas}) were compared among HC and PwMS, respectively, in PPMS and RRMS. Significance was set at $p < 0.05$. ß: beta regression; CI: confidence interval; GCIP: ganglion cell and inner plexiform layer; HC: healthy controls; INL: inner nuclear layer; LMU: Ludwig-Maximilians Universität München (Spectralis OCT); MSK: Marianne-Strauß-Klinik (Cirrus OCT); N (eyes): number of eyes included; ONPL: outer nuclear and outer plexiform layer; PPMS: primary-progressive multiple sclerosis; pRNFL: peripapillary retinal nerve fiber layer; PwMS: persons with multiple sclerosis (PPMS and RRMS); RRMS: relapsing–remitting multiple sclerosis; SD: standard deviation; SE: standard error; TMV: total macular volume. [1] Generalized linear mixed model using *gender* and *age at* OCT_{bas} as covariates to compare HC vs. PwMS. [2] Generalized linear mixed model using *gender*, *age at* OCT_{bas}, and *disease duration* (initial manifestation to OCT_{bas} in years) to compare MS subtypes.

2.3. Longitudinal Retinal Layer Analysis

For the longitudinal analysis of retinal layers, relative annual change rates were calculated (in %) (Table 3). A significantly higher annual decrease in the pRNFL thickness was detected in PwMS compared with HC (mean in %: −0.73 vs. −0.13; $p = 0.002$). The mean annual INL volume change significantly differed between HC and PwMS (mean in %: 1.21 vs. 0.33; $p = 0.005$), an additional age-related analysis for patients with RRMS or PPMS is provided in Supplement Figure S1. The comparison between patients with RRMS and PPMS disease courses showed no significant differences in the relative annual change rates. However, the mean decrease in the GCIP volume was higher in RRMS vs. PPMS (mean in %: −0.60 vs. −0.16; $p = 0.077$).

Table 3. Relative annual change rates of retinal layers.

	HC vs. PwMS				**PPMS vs. RRMS**			
	HC	**PwMS**	**ß (SE)**	***p*-Value [1]**	**PPMS**	**RRMS**	**ß (SE)**	***p*-Value [2]**
Peripapillary Scan, relative annual change (MSK and LMU)								
pRNFL mean in % (95% CI) N (eyes)	**−0.131** **(−0.436–0.174)** 102	**−0.730** **(−0.942–−0.519)** 208	***−0.600*** ***(0.191)***	***0.002***	−0.597 (−0.877–−0.317) 100	−0.833 (−1.103–−0.562) 108	*0.235* *(0.218)*	*0.282*
Macula Scan, relative annual change (LMU)								
TMV mean in % (95% CI) N (eyes)	−0.076 (−0.234–0.083) 110	−0.188 (−0.332–−0.044) 133	*−0.112* *(0.110)*	*0.309*	−0.226 (−0.417–−0.036) 61	−0.200 (−0.371–−0.028) 72	*−0.027* *(0.145)*	*0.854*
GCIP mean in % (95% CI) N (eyes)	−0.462 (−0.714–−0.209) 112	−0.372 (−0.602–−0.141) 133	*0.090* *(0.175)*	*0.608*	−0.160 (−0.486–0.166) 62	−0.601 (−0.892–−0.309) 71	*0.440* *(0.247)*	*0.077*
INL mean in % (95% CI) N (eyes)	**1.210** **(0.750–1.670)** 103	**0.326** **(−0.077–0.730)** 133	***−0.884*** ***(0.312)***	***0.005***	0.158 (−0.252–0.569) 61	0.248 (−0.122–0.618) 72	*−0.090* *(0.313)*	*0.775*
ONPL mean in % (95% CI) N (eyes)	−0.078 (−0.359–0.203) 112	−0.317 (−0.578–−0.056) 130	*−0.239* *(1.973)*	*0.226*	−0.312 (−0.640–0.016) 61	−0.308 (−0.613–−0.003) 69	*−0.004* *(0.253)*	*0.986*

Relative annual change rates of retinal layer thickness and volumes were compared among HC and PwMS, respectively, in PPMS and RRMS, after exclusion of extreme lower and upper outliers according to Tukey (1st quartile − 3xIQR < range included < 1st quartile + 3xIQR). Significance was set at $p < 0.05$. *ß*: beta regression; CI: confidence interval; GCIP: ganglion cell and inner plexiform layer; HC: healthy controls; INL: inner nuclear layer; LMU: Ludwig-Maximilians Universität München (Spectralis OCT); MSK: Marianne-Strauß-Klinik (Cirrus OCT); N (eyes): number of eyes included; ONPL: outer nuclear and outer plexiform layer; PPMS: primary-progressive multiple sclerosis; pRNFL: peripapillary retinal nerve fiber layer; PwMS: persons with multiple sclerosis (PPMS and RRMS); RRMS: relapsing–remitting multiple sclerosis; SD: standard deviation; SE: standard error; TMV: total macular volume. [1] Generalized linear mixed model using *gender* and *age at* OCT_{bas} as covariates to compare HC vs. PwMS. [2] Generalized linear mixed model using *gender*, *age at* OCT_{bas}, and *disease duration* (initial manifestation to OCT_{bas} in years) to compare MS subtypes.

2.4. Deterioration in Ambulatory Function Associates with Macular Layer Degeneration

Data on AS measured in routine clinical care were available from 87 PwMS for GpRNFL (PPMS $n = 37$; RRMS $n = 50$) with a median observation time of 37 months (IQR: 23.5–61) and 48 PwMS for macular layers (PPMS $n = 17$; RRMS $n = 31$) with a median observation time of 27 months (IQR: 18.75–42.5). A total of 16 of 37 patients with PPMS deteriorated (Table 1). A comparison of OCT parameters between RRMS and PPMS patients with stable AS during the observation period revealed no differences, apart from the relative atrophy rate of the GCIP, which was significantly increased in subjects with RRMS (p-value = 0.004) (Table 4). The eyes of the PPMS subjects with a deterioration in the AS (during OCT_{bas} to OCT_{lfu}) showed significantly higher mean relative annual decrease rates in the TMV, GCIP, and ONPL compared with eyes of PPMS subjects with stable AS (t-test: all p-value < 0.05; ANCOVA: all p-value < 0.05; all $r > 0.3$) (Table 4). For every −0.1% decrease in the TMV, GCIP, and ONPL, the risk of a deterioration in the AS increased by 31% (hazard ratio (HR): 1.309), 11% (HR: 1.112), and 16% (HR: 1.161), respectively, in PPMS (Table 5). Moreover, a deterioration in the EDSS in PPMS individuals was significantly associated with the relative annual atrophy rates in the pRNFL, TMV, and GCIP (all p-value < 0.05) (Table 5).

Table 4. Association between ambulation functional score and relative annual change rates of retinal layers.

				RRMS vs. PPMS Stable AS			PPMS Stable vs. Deterioration in AS		
	RRMS Stable AS (*t*-Test)	**PPMS Stable AS (*t*-Test)**	**PPMS Deterioration AS (*t*-Test)**	***p*-Value (*t*-Test)**	***p*-Value (ANCOVA)**	***r***	***p*-Value (*t*-Test)**	***p*-Value (ANCOVA)**	***r***
Peripapillary Scan (MSK and LMU)									
Relative annual change in pRNFL mean in %, (SD)	−0.766 (2.256)	−1.102 (1.797)	−0.656 (1.019)	0.365	*0.956*	*0.048*	*0.192*	0.362	*0.101*
Macula Scan (LMU)									
Relative annual change in TMV mean in %, (SD)	−0.186 (0.648)	0.001 (0.856)	−0.544 (0.688)	0.239	*0.987*	*0.002*	***0.025***	***0.032***	***0.310***
Relative annual change in GCIP mean in %, (SD)	−0.325 (0.912)	0.278 (1.640)	−1.012 (1.103)	0.060	***0.004***	***0.295***	***0.005***	***0.006***	***0.390***
Relative annual change in INL mean in % (SD)	0.451 (1.450)	0.724 (2.643)	−0.154 (0.878)	0.516	*0.681*	*0.043*	*0.179*	0.203	*0.187*
Relative annual change in ONPL mean in %, (SD)	−0.291 (1.631)	0.150 (1.672)	−0.979 (1.163)	0.223	*0.856*	*0.019*	***0.015***	***0.020***	***0.336***

The relative annual rates of change in the thickness and volumes of the retinal layers were compared within PwMS and PPMS only, graded by stable vs. deteriorated ambulation functional score over the study period. ANCOVA with covariates of *age at* OCT_{bas} and *gender*. No exclusion of outliers. Mean relative annual change rates for the ANCOVA analysis are not shown. *t*-Test stable RRMS vs. PPMS with AS deterioration with *p*-value = 0.008; ANCOVA with covariates of *age at* OCT_{bas} and *gender* for stable RRMS vs. PPMS with AS deterioration with *p*-value = 0.181 and *r* = 0.151. Significance was set at $p < 0.05$. AS: ambulation functional score; GCIP: ganglion cell and inner plexiform layer; INL: inner nuclear layer; LMU: Ludwig-Maximilians Universität München (Spectralis OCT); MSK: Marianne-Strauß-Klinik (Cirrus OCT); ONPL: outer nuclear and outer plexiform layer; pRNFL: peripapillary retinal nerve fiber layer; SD: standard deviation; TMV: total macular volume.

Table 5. Cox-regression analysis on effects of retinal layer atrophy rates on deterioration in the ambulation functional score and in the EDSS.

	Ambulation Functional Score				**EDSS**	
	All PwMS		**PPMS**		**PPMS**	
	HR (95% CI)	***p*-Value**	**HR (95% CI)**	***p*-Value**	**HR (95% CI)**	***p*-Value**
Relative annual atrophy rate of pRNFL (in ‰)	1.009 (0.979–1.040)	*0.550*	1.024 (0.992–1.057)	*0.143*	**1.021 (1.002–1.040)**	***0.030***
Relative annual atrophy rate of TMV (in ‰)	**1.265 (1.132–1.414)**	***<0.001***	**1.309 (1.155–1.483)**	***<0.001***	**1.172 (1.081–1.270)**	***<0.001***
Relative annual atrophy rate of GCIP (in ‰)	**1.093 (1.041–1.148)**	***<0.001***	**1.112 (1.053–1.174)**	***<0.001***	**1.059 (1.016–1.104)**	***0.007***
Relative annual atrophy rate of INL (in ‰)	1.017 (0.973–1.062)	*0.456*	1.026 (0.972–1.084)	*0.352*	1.004 (0.974–1.035)	*0.779*
Relative annual atrophy rate of ONPL (in ‰)	1.013 (1.001–1.025)	***0.036***	**1.161 (1.086–1.241)**	***<0.001***	1.026 (0.977–1.078)	*0.301*

The effect of the relative annual atrophy rates of retinal layers (*relative annual rates of change in retinal layers* x − 1; in ‰) on deterioration in the ambulation functional score (AS) in PwMS (RRMS and PPMS). The EDSS for PPMS subjects was evaluated using a Cox-regression model adjusted for *age at baseline OCT* (OCT_{bas}) and *gender*. No exclusion of outliers. Significance was set at $p < 0.05$. CI: confidence interval; EDSS: expanded disability status scale; GCIP: ganglion cell and inner plexiform layer; HR: hazard ratio; INL: inner nuclear layer; ONPL: outer nuclear and outer plexiform layer; pRNFL: peripapillary retinal nerve fiber layer; TMV: total macular volume.

3. Discussion

Disease progression in PwMS is currently assessed primarily based on medical history and by means of clinical tests, in particular the EDSS and the AS. However, clinical testing can be subject to variability due to external and individual causes, making it difficult to assess disease progression as an individual follow-up parameter. Our aim was to investigate OCT as a surrogate to assess MS progression. In patients with PPMS, we found an association of longitudinal retinal neuroaxonal layer-changes with walking capacity as assessed by the AS: PPMS individuals with AS worsening over the median observation period of 27 months had an increased retinal neuroaxonal volume loss of the TMV, GCIP, and ONPL, compared with PPMS persons with stable AS. Higher retinal atrophy rates were also associated with a deterioration in the EDSS. To the best of our knowledge, the association between walking ability and retinal neuroaxonal layer measurements has so far only been investigated cross-sectionally [18]. In that study, a significant association between slowed walking speed (measured with the timed 25-foot walk test, T25FW) and reduced TMV, but not pRNFL, was shown. This indicates, together with our results, that only the atrophy rates of the macular layers represent additional markers of disease progression. We emphasize that the interval censoring poses a limitation of our Cox-regression model.

In addition, we report cross-sectional and longitudinal analyses of the retinal layers in RRMS, PPMS, and HC: In our cross-sectional approach, we found a significantly reduced pRNFL thickness as well as reduced TMV and GCIP volumes in PwMS compared with HC. Retinal neuroaxonal degeneration is a well-studied finding in eyes of PwMS with or without optic neuritis [19,20]. However, we detected no significant differences between PPMS and RRMS in the cross-sectional analysis of retinal layers adjusted for age, gender, and disease duration. In our longitudinal analysis, using age and gender as covariates, we found an overall increased thinning of the pRFNL in PwMS vs. HC. Similar results have been repeatedly reported in previous studies [13,21]. Additionally, we detected a significant difference in the relative annual change rate of INL volume between PwMS and HC. We emphasize that several authors reported influencing factors on the INL analysis, including physiological variations [22], clinical MS activity during the observation period [23], and immunotherapy effects [24]. In addition, there is an ongoing debate about the INL change rate in relation to age and MS disease duration [13,25–27]. In our cohort, we observed

swelling of the INL in younger PwMS, whereas INL thinning occurred with age. In summary, our results support the hypothesis of Cordano et al., interpreting the change rate of INL in PwMS as *early inflammation followed by later neurodegeneration* [25]. As caveats, we state that we report on INL volumes, while INL thickness rates of change have been reported in the cited literature [13,25]. Further, our analyzed cohorts differ significantly in demographic and clinical parameters. Within our analyzed cohorts, we did not detect any significant differences in the rates of change of the retinal layers between PPMS and RRMS.

The main result of our investigation is the association between gait deterioration and increased longitudinal atrophy rates of retinal layers in PPMS. OCT might therefore provide imaging markers to assess disease progression in PwMS in the future. Further, we would like to emphasize the long duration of observation, especially of the progressive MS subjects in our cohort. Limitations result from the retrospective approach and the resulting restrictions on data availability, the different devices used for OCT examinations, and the reduced sample size of PwMS with available data on ambulatory performances (AS). Also, based on the retrospective analysis, it cannot be excluded that subclinical comorbidities also have an influence on the measured neuroaxonal degeneration of the retina, which underlines the explorative approach of this analysis. A prospective, multicenter study with a structured homogenized clinical dataset is needed for further analysis between walking ability and macular degeneration in PwMS.

4. Materials and Methods

4.1. Study Design

For the analysis, we retrospectively created a joint dataset from two large MS centers in southern Germany: (i) Institute of Clinical Neuroimmunology, Ludwig-Maximilians-Universität München, Munich (tertiary center; LMU Hospital) and (ii) Marianne-Strauß-Klinik, Treatment Center Kempfenhausen for Patients with Multiple Sclerosis, Berg (secondary center; MSK). Inclusion criteria were (i) all PwMS (RRMS and PPMS) with the presence of at least two OCT examinations with an interval of at least six months; (ii) no history of or occurrence of optic neuritis in the observation period; (iii) age >18 years at OCT_{bas}. OCT examinations were performed from 2011 to 2022 as part of routine clinical care. Diagnoses of RRMS and PPMS were made according to the revised McDonald criteria 2017 [28]. Exclusion criteria were (i) eyes with anamnestic history of optic neuritis; (ii) eyes with a refraction error > 5 diopters; (iii) patients with a history of a known disease affecting the visual system. If available, we considered the maximum walking distance in PwMS (up to 500 m) on the dates of OCT_{bas} and the last follow-up OCT examination (OCT_{lfu}), using the AS (Neurostatus Version 04/10.2 modified from [29,30]) in a binary manner (improved/stable vs. deterioration). In PPMS subjects with available AS data, the EDSS was also evaluated accordingly. RRMS subjects with an AS deterioration possibly due to, or as part of a relapse during the observation period (n = 9 patients), were excluded from further analysis to evaluate the association of OCT parameters and relapse-independent progression in ambulatory function. Next to the mentioned inclusion/exclusion criteria, HC had no diagnosed neurological or ophthalmological disease. All individuals examined at LMU gave written consent, and the retrospective data of the individuals included from MSK were irreversibly anonymized. The local ethic committee gave approval for a retrospective analysis of OCT datasets (project number: 19-570). This study was conducted according to the Declaration of Helsinki.

4.2. Optical Coherence Tomography (OCT)

Spectral domain OCT examinations were performed using a Spectralis SD-OCT at LMU (Heidelberg Engineering, Heidelberg, Germany, OCT2-Module, automated retinal layer segmentation by Heyex v2.5.5, Heidelberg Engineering, Heidelberg, Germany) and a Cirrus HD-OCT 4000 at MSK (Carl Zeiss Meditec, Jena, Germany, version 8.1.0.117). A 3 mm ring scan centered on the optic nerve head was performed to assess the peripapillary retinal nerve fiber layer (pRNFL) thickness (in µm). The pRNFL thickness was analyzed for

cohorts from both centers after including a conversion factor [31]. In addition, the volumes (mm^3) of four retinal layers acquired from a macula scan (25 [30 × 25°, ART 13] vertical b-scans) were evaluated only for subjects examined at LMU (6 mm ring centered on the fovea, not available for the MSK): (i) total macular volume (TMV); (ii) combined ganglion cell and inner plexiform layer (GCIP), (iii) inner nuclear layer (INL); (iv) combined outer plexiform and outer nuclear layer (ONPL) (Figure 1). As far as possible considering the listed inclusion and exclusion criteria, both eyes of one person were analyzed.

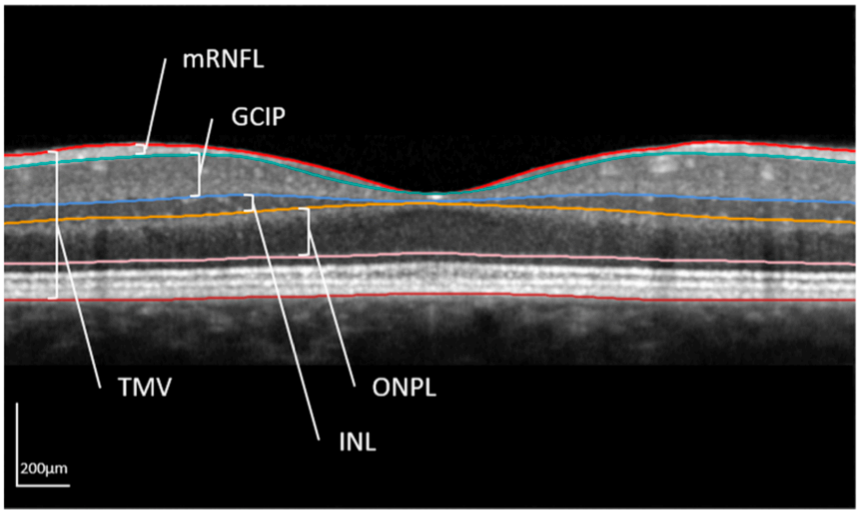

Figure 1. Macula scan in optical coherence tomography.

The different layers are shown in a horizontal OCT scan centered on the middle of the fovea. The layer segmentation is done automatically by the segmentation tool of Heyex v2.5.5. Analyzed retinal structures of this work were the total macular volume (TMV); combined ganglion cell and inner plexiform layer (GCIP), inner nuclear layer (INL); and combined outer nuclear and outer plexiform layer (ONPL). Additionally, the macular retinal nerve fiber layer (mRNFL) is shown. However, in the present analysis, the peripapillary RNFL (pRNFL) determined with a 3 mm ring scan centered on the optic disc was evaluated (in µm).

4.3. Statistical Analysis

SPSS Statistics 27 (IBM, Armonk, New York, United States of America) was used for statistical analysis. For comparison of nominally distributed features the Chi-squared-test was used, for metric data the *t*-test was applied, if normally distributed, otherwise the Kruskal-Wallis-test. A generalized mixed linear model was performed to evaluate the OCT parameters cross-sectionally (at OCT_{bas}) and longitudinally (relative annual change rates) between cohorts: (i) HC vs. PwMS: Here, *gender* and *age at* OCT_{bas} were considered as covariates; (ii) PPMS vs. RRMS: Additionally, the *disease duration* (years from initial manifestation to OCT_{bas}) was considered. By including a random effect for the *centers*, we could not determine a high variance between the centers. Therefore, *center* was not included as a random variable. For the analysis of relative annual rates of change in retinal layers, extreme outliers were excluded according to Tukey (1st quartile – 3xIQR < range included < 3rd quartile + 3xIQR; interquartile range (IQR)) [32]. A *t*-test and an ANCOVA analysis (covariates *gender* and *age at* OCT_{bas}) were used to assess associations between AS and change rates of retinal layers. Further, a Cox-regression (covariates *gender* and *age*

at OCT_{bas}) was performed to evaluate the effect of relative annual atrophy rates of retinal layers (*relative annual rates of change in retinal layers*x − 1; in ‰) on deterioration in the AS in PwMS. In PPMS subjects, also a Cox-regression (covariates *gender* and *age at* OCT_{bas}) was performed to evaluate the effect of relative annual atrophy rates of retinal layers (*relative annual rates of change in retinal layers*x − 1; in ‰) on deterioration in the EDSS. Significance was set at $p < 0.05$.

Supplementary Materials: The following supporting information can be downloaded at https://www.mdpi.com/article/10.3390/ijms241612872/s1.

Author Contributions: Conceptualization: I.K. and J.H.; Methodology: T.K., I.K. and J.H.; Formal analysis: J.A.G., L.B. and S.B.; Investigation: L.B. and M.S.; Writing—original draft preparation: J.A.G.; Writing—review and editing: L.B., S.B., M.S., T.K., I.K. and J.H.; Supervision: I.K. and J.H. All authors have read and agreed to the published version of the manuscript.

Funding: This research received no external targeted funding.

Institutional Review Board Statement: This study was conducted in accordance with the Declaration of Helsinki and approved by the Institutional Review Board (or Ethics Committee) of Ludwig-Maximilians-Universität München, Munich, Germany (protocol code 19-570 on 12 August 2019).

Informed Consent Statement: All individuals examined at LMU gave written consent, and the retrospective data of the individuals included from MSK were irreversibly anonymized.

Data Availability Statement: The data presented in this study are available on reasoned request from the corresponding author if the data exchange is possible with respect to valid data protection laws.

Acknowledgments: J.A.G. received a research grant from the Deutsche Forschungsgemeinschaft (DFG, German Research Foundation; SFB/TRR 274, ID 408885537). L.B. received a research scholarship from Ludwig-Maximilians-Universität München, Munich, Germany. This work is part of the medical thesis of L.B. at the Ludwig-Maximilians-Universität München, Munich, Germany.

Conflicts of Interest: S.B. and M.S. have nothing to disclose. J.A.G. reports travel expenses and non-financial support from Merck, outside the submitted work. T.K. has received speaker honoraria and/or personal fees for advisory boards from Novartis Pharma, Roche Pharma, Alexion/Astra Zeneca, and Biogen; the institution she works for has received grant support for her research from Bayer-Schering A.G., Novartis, and Chugai Pharma. I.K. has received personal compensation for consulting, serving on a scientific advisory board, speaking, and other activities with Alexion, Almirall, Bayer, Biogen, Hexal, Horizon, Merck, Neuraxpharm, Roche/Chugai, and Sanofi. I.K. is an editorial board member of BMC Neurology, Frontiers in Neurology, and Frontiers in Immunology. J.H. reports grants from Friedrich-Baur-Stiftung, Merck, and Horizon; personal fees and non-financial support from Alexion, Horizon, Roche, Merck, Novartis, Biogen, B.M.S., and Janssen; and non-financial support from the Guthy-Jackson Charitable Foundation and The Sumaira Foundation.

References

1. Albrecht, H.; Wötzel, C.; Erasmus, L.P.; Kleinpeter, M.; König, N.; Pöllmann, W. Day-to-day variability of maximum walking distance in MS patients can mislead to relevant changes in the Expanded Disability Status Scale (EDSS): Average walking speed is a more constant parameter. *Mult. Scler. J.* **2001**, *7*, 105–109. [CrossRef] [PubMed]
2. Sandroff, B.M.; Sosnoff, J.J.; Motl, R.W. Physical fitness, walking performance, and gait in multiple sclerosis. *J. Neurol. Sci.* **2013**, *328*, 70–76. [CrossRef] [PubMed]
3. Scholz, M.; Haase, R.; Trentzsch, K.; Weidemann, M.L.; Ziemssen, T. Fear of falling and falls in people with multiple sclerosis: A literature review. *Mult. Scler. Relat. Disord.* **2020**, *47*, 102609. [CrossRef] [PubMed]
4. Petzold, A.; Balcer, L.J.; Calabresi, P.A.; Costello, F.; Frohman, T.C.; Frohman, E.M.; Martinez-Lapiscina, E.H.; Green, A.J.; Kardon, R.; Outteryck, O.; et al. Retinal layer segmentation in multiple sclerosis: A systematic review and meta-analysis. *Lancet Neurol.* **2017**, *16*, 797–812. [CrossRef]
5. Balk, L.J.; Cruz-Herranz, A.; Albrecht, P.; Arnow, S.; Gelfand, J.M.; Tewarie, P.; Killestein, J.; Uitdehaag, B.M.; Petzold, A.; Green, A.J. Timing of retinal neuronal and axonal loss in MS: A longitudinal OCT study. *J. Neurol.* **2016**, *263*, 1323–1331. [CrossRef]
6. Klumbies, K.; Rust, R.; Dörr, J.; Konietschke, F.; Paul, F.; Bellmann-Strobl, J.; Brandt, A.U.; Zimmermann, H.G. Retinal Thickness Analysis in Progressive Multiple Sclerosis Patients Treated with Epigallocatechin Gallate: Optical Coherence Tomography Results From the SUPREMES Study. *Front. Neurol.* **2021**, *12*, 615790. [CrossRef]

7. Balk, L.J.; Tewarie, P.; Killestein, J.; Polman, C.H.; Uitdehaag, B.; Petzold, A. Disease course heterogeneity and OCT in multiple sclerosis. *Mult. Scler. J.* **2014**, *20*, 1198–1206. [CrossRef]
8. Behbehani, R.; Abu Al-Hassan, A.; Al-Salahat, A.; Sriraman, D.; Oakley, J.D.; Alroughani, R. Optical coherence tomography segmentation analysis in relapsing remitting versus progressive multiple sclerosis. *PLoS ONE* **2017**, *12*, e0172120. [CrossRef]
9. Behbehani, R.; Adnan, H.; Al-Hassan, A.A.; Al-Salahat, A.; Alroughani, R. Predictors of retinal atrophy in multiple sclerosis: A longitudinal study using spectral domain optical coherence tomography with segmentation analysis. *Mult. Scler. Relat. Disord.* **2018**, *21*, 56–62. [CrossRef]
10. Henderson, A.P.; Trip, S.A.; Schlottmann, P.G.; Altmann, D.R.; Garway-Heath, D.F.; Plant, G.T.; Miller, D.H. An investigation of the retinal nerve fibre layer in progressive multiple sclerosis using optical coherence tomography. *Brain* **2008**, *131 Pt 1*, 277–287. [CrossRef]
11. Henderson, A.P.; Trip, S.A.; Schlottmann, P.G.; Altmann, D.R.; Garway-Heath, D.F.; Plant, G.T.; Miller, D.H. A preliminary longitudinal study of the retinal nerve fiber layer in progressive multiple sclerosis. *J. Neurol.* **2010**, *257*, 1083–1091. [CrossRef]
12. Petracca, M.; Sumowski, J.; Fabian, M.; Miller, A.; Lublin, F.; Inglese, M. Looking into cognitive impairment in primary-progressive multiple sclerosis. *Eur. J. Neurol.* **2017**, *25*, 192–195. [CrossRef]
13. Sotirchos, E.S.; Gonzalez Caldito, N.; Filippatou, A.; Fitzgerald, K.C.; Murphy, O.C.; Lambe, J.; Nguyen, J.; Button, J.; Ogbuokiri, E.; Crainiceanu, C.M.; et al. Progressive Multiple Sclerosis Is Associated with Faster and Specific Retinal Layer Atrophy. *Ann. Neurol.* **2020**, *87*, 885–896. [CrossRef]
14. Bsteh, G.; Hegen, H.; Altmann, P.; Auer, M.; Berek, K.; Di Pauli, F.; Haider, L.; Kornek, B.; Krajnc, N.; Leutmezer, F.; et al. Retinal layer thickness predicts disability accumulation in early relapsing multiple sclerosis. *Eur. J. Neurol.* **2023**, *30*, 1025–1034. [CrossRef] [PubMed]
15. Waldman, A.T.; Hiremath, G.; Avery, R.A.; Conger, A.; Pineles, S.L.; Loguidice, M.J.; Talman, L.S.; Galetta, K.M.; Shumski, M.J.; Wilson, J.; et al. Monocular and binocular low-contrast visual acuity and optical coherence tomography in pediatric multiple sclerosis. *Mult. Scler. Relat. Disord.* **2013**, *3*, 326–334. [CrossRef] [PubMed]
16. Rosenkranz, S.C.; Gutmann, L.; Has Silemek, A.C.; Dorr, M.; Häußler, V.; Lüpke, M.; Mönch, A.; Reinhardt, S.; Kuhle, J.; Tilsley, P.; et al. Visual function resists early neurodegeneration in the visual system in primary progressive multiple sclerosis. *J. Neurol. Neurosurg. Psychiatry* 2023, *online ahead of print*. [CrossRef]
17. Mirmosayyeb, O.; Zivadinov, R.; Weinstock-Guttman, B.; Benedict, R.H.B.; Jakimovski, D. Optical coherence tomography (OCT) measurements and cognitive performance in multiple sclerosis: A systematic review and meta-analysis. *J. Neurol.* **2023**, *270*, 1266–1285. [CrossRef] [PubMed]
18. Balantrapu, S.; Sandroff, B.M.; Pula, J.H.; Motl, R.W. Integrity of the anterior visual pathway and its association with ambulatory performance in multiple sclerosis. *Mult. Scler. Int.* **2013**, *2013*, 481035. [CrossRef]
19. Sepulcre, J.; Murie-Fernandez, M.; Salinas-Alaman, A.; García-Layana, A.; Bejarano, B.; Villoslada, P. Diagnostic accuracy of retinal abnormalities in predicting disease activity in MS. *Neurology* **2007**, *68*, 1488–1494. [CrossRef]
20. Coric, D.; Balk, L.J.; Uitdehaag, B.M.J.; Petzold, A. Diagnostic accuracy of optical coherence tomography inter-eye percentage difference for optic neuritis in multiple sclerosis. *Eur. J. Neurol.* **2017**, *24*, 1479–1484. [CrossRef]
21. Abalo-Lojo, J.M.; Treus, A.; Arias, M.; Gómez-Ulla, F.; Gonzalez, F. Longitudinal study of retinal nerve fiber layer thickness changes in a multiple sclerosis patients cohort: A long term 5 year follow-up. *Mult. Scler. Relat. Disord.* **2018**, *19*, 124–128. [CrossRef] [PubMed]
22. Nij Bijvank, J.A.; Uitdehaag, B.M.J.; Petzold, A. Interpretation of Longitudinal Changes of the Inner Nuclear Layer in MS. *Ann. Neurol.* **2022**, *92*, 154–155. [CrossRef] [PubMed]
23. Balk, L.J.; Coric, D.; Knier, B.; Zimmermann, H.G.; Behbehani, R.; Alroughani, R.; Martinez-Lapiscina, E.H.; Brandt, A.U.; Sánchez-Dalmau, B.; Vidal-Jordana, A.; et al. Retinal inner nuclear layer volume reflects inflammatory disease activity in multiple sclerosis; a longitudinal OCT study. *Mult. Scler. J. Exp. Transl. Clin.* **2019**, *5*, 2055217319871582. [CrossRef] [PubMed]
24. Miscioscia, A.; Puthenparampil, M.; Miante, S.; Pengo, M.; Rinaldi, F.; Perini, P.; Gallo, P. Retinal inner nuclear layer thinning is decreased and associates with the clinical outcome in ocrelizumab-treated primary progressive multiple sclerosis. *J. Neurol.* **2022**, *269*, 5436–5442. [CrossRef] [PubMed]
25. Cordano, C.; Yiu, H.H.; Oertel, F.C.; University of California, San Francisco MS-EPIC Team; Gelfand, J.M.; Hauser, S.L.; Cree, B.A.C.; Green, A.J. Retinal INL Thickness in Multiple Sclerosis: A Mere Marker of Neurodegeneration? *Ann. Neurol.* **2021**, *89*, 192–193. [CrossRef] [PubMed]
26. Sotirchos, E.S.; Calabresi, P.A.; Saidha, S. Reply to "Retinal INL Thickness in Multiple Sclerosis: A Mere Marker of Neurodegeneration?". *Ann. Neurol.* **2021**, *89*, 193–194. [CrossRef]
27. Cordano, C.; Yiu, H.H.; Abdelhak, A.; Beaudry-Richard, A.; Oertel, F.C.; Green, A.J. Reply to "Interpretation of Longitudinal Changes of the Inner Nuclear Layer in MS". *Ann. Neurol.* **2022**, *92*, 156. [CrossRef]
28. Thompson, A.J.; Banwell, B.L.; Barkhof, F.; Carroll, W.M.; Coetzee, T.; Comi, G.; Correale, J.; Fazekas, F.; Filippi, M.; Freedman, M.S.; et al. Diagnosis of multiple sclerosis: 2017 revisions of the McDonald criteria. *Lancet Neurol.* **2018**, *17*, 162–173. [CrossRef]
29. Kurtzke, J.F. Rating neurologic impairment in multiple sclerosis: An expanded disability status scale (EDSS). *Neurology* **1983**, *33*, 1444–1452. [CrossRef]
30. Available online: https://www.neurostatus.net/media/specimen/Definitions_0410-2_s.pdf (accessed on 1 July 2023).

31. Kenney, R.C.; Liu, M.; Hasanaj, L.; Joseph, B.; Abu Al-Hassan, A.; Balk, L.J.; Behbehani, R.; Brandt, A.; Calabresi, P.A.; Frohman, E.; et al. The Role of Optical Coherence Tomography Criteria and Machine Learning in Multiple Sclerosis and Optic Neuritis Diagnosis. *Neurology* **2022**, *99*, e1100–e1112. [CrossRef]
32. Tukey, J.W. *Exploratory Data Analysis*; Pearson: London, UK, 1977; Volume 2.

8. Veröffentlichung II

frontiers in Neurology

ORIGINAL RESEARCH
published: 10 December 2021
doi: 10.3389/fneur.2021.780624

Optical Coherence Tomography to Assess Neurodegeneration in Phenylalanine Hydroxylase Deficiency

Amelie S. Lotz-Havla[1], Katharina Weiß[1], Katharina Schiergens[1], Stephanie Regenauer-Vandewiele[1], Klaus G. Parhofer[2], Tara Christmann[3], Luise Böhm[3], Joachim Havla[3,4†] and Esther M. Maier[1*†]*

[1] Dr. von Hauner Children's Hospital, LMU University Hospital, Ludwig-Maximilians-Universität München, Munich, Germany, [2] Medical Department IV - Grosshadern, LMU University Hospital, Ludwig-Maximilians-Universität München, Munich, Germany, [3] Institute of Clinical Neuroimmunology, LMU University Hospital, Ludwig-Maximilians-Universität München, Munich, Germany, [4] Data Integration for Future Medicine (DIFUTURE) Consortium, Ludwig-Maximilians-Universität München, Munich, Germany

OPEN ACCESS

Edited by:
Philipp Albrecht,
Heinrich Heine University of Düsseldorf, Germany

Reviewed by:
Olivier Outteryck,
Université de Lille, France
Vincenzo Parisi,
Fondazione G.B. Bietti (IRCCS), Italy

***Correspondence:**
Joachim Havla
joachim.havla@med.uni-muenchen.de
Esther M. Maier
esther.maier@med.uni-muenchen.de

[†]These authors have contributed equally to this work and share last authorship

Specialty section:
This article was submitted to Multiple Sclerosis and Neuroimmunology, a section of the journal Frontiers in Neurology

Received: 21 September 2021
Accepted: 02 November 2021
Published: 10 December 2021

Citation:
Lotz-Havla AS, Weiß K, Schiergens K, Regenauer-Vandewiele S, Parhofer KG, Christmann T, Böhm L, Havla J and Maier EM (2021) Optical Coherence Tomography to Assess Neurodegeneration in Phenylalanine Hydroxylase Deficiency. Front. Neurol. 12:780624. doi: 10.3389/fneur.2021.780624

In phenylalanine hydroxylase (PAH) deficiency, an easily feasible method to access the progression of neurodegeneration is warranted to contribute to current discussions on treatment indications and targets. The objective of the present study was to investigate whether optical coherence tomography (OCT) measures as markers of neurodegeneration differ between patients with PAH deficiency and healthy controls (HCs) according to phenotype and metabolic control. In this single-center cross-sectional study, 92 patients with different phenotypes of PAH deficiency [PAH deficiency not requiring treatment, early treated phenylketonuria (ETPKU), and late-diagnosed phenylketonuria (PKU)] compared with 76 HCs were examined using spectral-domain OCT. Indices of phenylalanine elevation and variability were correlated with OCT parameters. Late-diagnosed PKU patients showed reduced peripapillary retinal nerve fiber layer (pRNFL) thickness and combined ganglion cell and inner plexiform layer (GCIPL) volume. Adult ETPKU patients were found to have lower GCIPL volume ($p = 0.016$), which correlated with the indices of phenylalanine control. In pediatric ETPKU patients with poor metabolic control, pRNFL was significantly reduced ($p = 0.004$). Patients with PAH deficiency not requiring treatment did not exhibit retinal degeneration. Inner nuclear layer (INL) was significantly increased in the pediatric ETPKU patients, driven by those with current poor metabolic control ($p = 0.006$). Our data provide evidence of retinal neuroaxonal degeneration and INL swelling, depending on the phenotype, current age, and metabolic control. These findings suggest that OCT is suitable to investigate neurodegeneration in PKU and we propose OCT as a sensitive, reliable, safe, low-burden, and low-cost examination for future multicenter studies.

Keywords: phenylketonuria, PKU, phenylalanine hydroxylase deficiency, optical coherence tomography, OCT, retinal neuroaxonal degeneration, neurodegeneration

INTRODUCTION

Phenylalanine hydroxylase (PAH) deficiency (OMIM #261600) is caused by autosomal recessive variants in the phenylalanine hydroxylase (*PAH*) gene and leads to an impaired degradation of the amino acid phenylalanine (Phe) to tyrosine and, as a consequence, to elevated concentrations of Phe in blood (1). According to current recommendations, PAH deficiency is classified as PAH deficiency not requiring treatment and PAH deficiency requiring treatment (hereinafter referred to as phenylketonuria, PKU) (2).

If untreated, PKU leads to severe brain damage with intellectual disability, seizures, and spasticity (3). This severe clinical phenotype is avoided by the introduction of newborn screening enabling an early initiation of dietary therapy to lower Phe concentrations in blood (4). Lately, the approvals of BH_4 (Kuvan®; sapropterin dihydrochloride), the natural cofactor of PAH, for BH_4-responsive patients and pegvaliase-pqpz (Palynziq®), a recombinant phenylalanine ammonia lyase, for adolescent and adult patients have expanded the treatment options for PKU, and thereby reduced the burden of a strict low-Phe diet for at least some of the patients (1, 5–9).

Despite these advances, data regarding the optimal treatment targets for PKU patients are insufficient leading to different treatment recommendations worldwide (2, 10). Additionally, there is only consensus that patients with Phe concentrations above 600 μmol/L do require treatment (2), and individuals with Phe concentrations below 360 μmol/L do not (2, 11). However, it remains under debate whether treatment is indicated in individuals with Phe concentrations between 360 and 600 μmol/L (2, 12–16). Neither neurocognitive nor MRI outcome studies have yet contributed to a clear decision on these issues.

White matter lesions (WMLs) have described as a marker of disease progression in PKU (17, 18). The extent of WMLs has been shown to be associated with the patient's age and metabolic control (17, 19–22). In untreated PKU patients, hypomyelination has been attributed to WMLs (17, 23, 24). In early treated PKU patients (ETPKU), WMLs are likely to reflect intramyelinic edema (17, 25) that can be reversed with re-adherence to a strict low-Phe diet (25, 26).

To address these unanswered questions, a monitoring test to assess the progression of neurodegeneration that is safe, low burden, and low-cost for the patients would be helpful.

Optical coherence tomography (OCT) is a non-invasive examination technique of the retina that allows the assessment of retinal neuroaxonal degeneration (27). OCT measurements have been identified as marker of disease progression in different (28–31) and neurodegenerative disorders (32, 33), as well as in metabolic neurodegenerative diseases, such as Wilson disease (34) and Niemann-Pick disease type C (35, 36).

Only recently, conflicting results of OCT studies on ETPKU cohorts have been described (37–40). Hopf et al. did not find any pathologies in the OCT measurements of the macula and optic nerve head in 10 pediatric and 9 adult PKU patients (37), whereas two other studies found evidence of retinal axonal degeneration in early treated pediatric (38) and adult PKU patients (39), as well as retinal neuronal degeneration in the early treated adult PKU patients (40).

To test the hypothesis that OCT is suitable to detect neurodegeneration in PAH deficiency, the present study investigated neuroaxonal retinal degeneration in patients with PAH deficiency according to phenotype and metabolic control. For this, (i) a large pediatric and adult cohort covering the entire phenotypic spectrum, from PAH deficiency not requiring treatment, over ETPKU to severely affected late-diagnosed PKU patients, was analyzed in comparison with the healthy controls (HCs), and (ii) the correlation of OCT measures with Phe elevation and variation was assessed. Beyond this, given the presumed WMLs pathology in ETPKU, the retinal correlate of cerebral intramyelinic edema was examined by analysis of the inner nuclear layer.

MATERIALS AND METHODS

Study Population

All registered patients who were diagnosed with PAH deficiency during neonatal or selective screening, and who were under regular care at the metabolic center of the LMU Hospital, Ludwig-Maximilians-University in Munich, Germany were invited to participate in this study. The inclusion criteria were confirmed PAH deficiency and age 6 years and older. The exclusion criteria were: (i) ocular comorbidities potentially confounding interpretation of OCT results ($> \pm 5.5$ diopters of spherical equivalent, $> \pm 3$ diopters of astigmatism, history of ocular disease, e.g., macular degeneration, glaucoma, and intracranial hypertension), (ii) history of systemic disease known to affect the retina [e.g., diabetes (41, 42)], (iii) history of any neurological disease unrelated to PAH deficiency, (iv) prematurity <36 weeks of gestational age (43), (v) current pregnancy (44), and (vi) interfering medical treatment. The exclusion criteria were identified based on the medical history of patients.

In this study, 150 eligible patients were prospectively identified and approached about the possibility of study participation. Ninety-five patients decided to participate, and of these 92 patients could be prospectively included in the study between October 2018 and January 2021 (as shown in **Table 1**). Three patients could not be included due to exclusion criteria (history of bilateral chorioretinitis, glaucoma, and $> \pm 5.5$ diopters of spherical equivalent).

Patients with PAH deficiency were classified as follows: patients requiring treatment ($N = 74$) and patients not requiring treatment ($N = 18$) (2, 45). The indication for treatment was based on the German recommendations at the time of diagnosis (46), i.e., therapy was initiated when Phe concentrations in the untreated patients exceeded 600 μmol/L. Patients with PAH deficiency requiring treatment were further divided into ETPKU and late-diagnosed PKU patients. The ETPKU group ($N = 70$) comprised patients who were diagnosed by neonatal screening. The group of late-diagnosed PKU patients ($N = 4$, age at diagnosis mean 22 months, SD 5.8 months, range 12–30 months) included patients who did not undergo newborn screening and were thus diagnosed and treated after the onset of symptoms.

TABLE 1 | Demographic information of cohorts and phenylalanine indices of the phenylalanine hydroxylase (PAH) deficient patient groups.

	HC		PAH deficient patients					
	(*N* = 76)		Not requiring treatment (*N* = 18)		ETPKU (*N* = 70)		PKU, late diagnosed (*N* = 4)	
	Mean	SD	Mean	SD	Mean	SD	Mean	SD
Age in years (range)	33 (7–59)	15	19 (7–50)	12	21 (7–54)	11	47 (20–59)	18
Gender f/m	50/26		14/4		41/29		3/1	
Blood Phe [μmol/l]								
Childhood (0–10 years)								
IDC			238	101	259	95	192	102
Average of yearly SD			55	25	155	53	226	64
Adolescence (11–16 years)								
IDC			269	128	498	208	586	354
Average of yearly SD			49	28	157	60	146	25
Adulthood (17 years +)								
IDC			269	106	662	313	645	261
Average of yearly SD			55	44	145	66	196	35
Lifetime								
IDC			238	88	405	212	581	276
Mean Phe			232	79	382	184	534	248
Mean exposure			−0.99	1.11	−0.01	1.38	3.90	2.94
Average of yearly SD			55	29	150	48	199	29
SD Phe			68	31	249	105	290	59
SD exposure			−1.55	0.96	0.30	1.40	3.00	2.10
Current Phe			n.a.	n.a.	552	404	948	626

IDC, average of yearly median phenylalanine levels; Phe, phenylalanine; HC, healthy control; PAH, phenylalanine hydroxylase; PKU, phenylketonuria; n.a., not applicable.

Seventy-six HCs matched for age and gender of the patients were also included in the study.

The study was performed in accordance with the Helsinki II Declaration and approved by the ethics committee of the Ludwig-Maximilians-University of Munich, Medical Faculty (part of project no 18-256). All the participants and/or their legal representatives gave written informed consent.

Spectral-Domain OCT

Optical coherence tomography examination was performed using a SD-OCT (Spectralis, Heidelberg Engineering, Heidelberg, Germany) with automatic real-time (ART) function for image averaging. Data are reported for peripapillary retinal nerve fiber layer thickness (pRNFL) to assess axonal degeneration. Total macular volume (TMV), volumes of combined ganglion cell and inner plexiform layer (GCIPL = GCL + IPL), and inner retinal layer (IRL = GCL + IPL + mRNFL) were assessed as markers for neuronal degeneration. Data for inner nuclear layer (INL) were evaluated to detect edema-related retinal changes. Calculation of macular layers is given for a 3 mm diameter cylinder around the fovea from a macular volume scan (20° × 20°, 25 vertical B-scans, ART ≤ 49). The pRNFL was measured with an activated eye tracker using 3.4 mm ring scans around the optic nerve (12°, 1,536 A-scans, ART ≤ 100). Segmentation of all the layers was performed semi-automatically using software provided by the OCT manufacturer (Eye Explorer 1.9.10.0 with viewing module 6.3.4.0, Heidelberg Engineering, Heidelberg, Germany). All the scans were checked for sufficient quality and segmentation errors and corrected, if necessary. OCT data are reported according to the APOSTEL and OSCAR-Ib recommendations (47–49). Data were analyzed separately for the patients up to 17 years of age and adults.

Indices of Metabolic Control

For all PAH deficient patients, comprehensive Phe monitoring data were available. Limited data were available for the patients who were treated at other metabolic centers in childhood ($N = 9$) or had poor adherence in adulthood ($N = 2$). To calculate the indices of Phe control, we combined previously proposed approaches (19, 50, 51). We averaged Phe control in the following age bands: childhood 0–10 years of age, adolescence 11–16 years of age, adulthood 17 years of age to present, and lifetime. For each age band, we considered the two measures Phe average and Phe variation (50). The Phe average was calculated by averaging the yearly median Phe levels (IDC). The Phe variation was calculated by averaging the SD for each year (50). We furthermore calculated the mean (mean Phe) and SD (SD Phe) of all available Phe levels for each patient (19). To take into account the duration (i.e., years) and accumulative effects of exposure to elevations

and variability in Phe, we calculated mean exposure and SD exposure as previously described (19). Furthermore, we considered the current Phe level determined at the time of OCT examination.

Statistical Analyses

The statistical analyses were performed using SPSS Statistics 26 (IBM, NY, USA) by the authors (ASL-H). Comparison of demographic data between the patient and control group was analyzed by using the chi-square test. Both eyes of each subject were included in the analysis as statistically dependent duplicates. Data were analyzed for normal distribution using a Shapiro–Wilk test and a Q-Q plot. To compare the PKU patients disease with controls, an unpaired *t*-test was used. To correct for multiple comparisons in the subgroup analysis, ANOVA with the Games-Howell *post-hoc* test was applied. The *p*-values below 0.05 were considered significant. A Pearson correlation analysis was performed to analyze the linear correlations of OCT parameters and indices of Phe control. Curve fitting using regression analysis and visual inspection of scatter plots after Locally Weighted Scatterplot Smoothing (LOESS) smoothing was applied to assess the relationship of variables in a correlation analysis. The subjects with missing data were excluded from the respective analysis. For two reasons, the correlation analyses were performed only for the group of adults aged 18–33 years ($N = 32$): (i) as expected from the literature (52), GCIPL volume was not associated with age in this cohort, and (ii) most comprehensive documentation of Phe levels was available.

RESULTS

Patient Characteristics and Indices of Metabolic Control

Table 1 shows demographic data of age, gender, and Phe control. On average, the ETPKU patients and the late-diagnosed PKU patients showed a good Phe control in childhood and adolescence (2). In adult age, IDC was slightly above the recommendation of <600 μmol/L (2) (ETPKU 662 μmol/L and late-diagnosed PKU 645 μmol/L). Variability in Phe was largely consistent across all age ranges.

The ETPKU cohort was further subdivided based on the average Phe levels as follows: ETPKU patients whose Phe levels were always within recommendations (ETPKU1: $N = 41$, IDC childhood 227 ± 52 μmol/L, IDC adolescence 358 ± 105 μmol/L, and IDC adulthood 416 ± 147 μmol/L) and ETPKU patients whose Phe levels were outside recommendations in childhood, adolescence, and/or adulthood (ETPKU2: $N = 29$, IDC childhood 305 ± 123 μmol/L, IDC adolescence 644 ± 188 μmol/L, and IDC adulthood 838 ± 280 μmol/L) (2).

Among 70 ETPKU patients, 36 (51%) were BH_4 responsive and treated with BH_4, alone or in combination with dietary therapy. Of note, BH_4 responsive patients showed significantly lower Phe concentrations after the relaxation of treatment suggested in adolescence as compared with BH_4 non-responsive patients (**Table 2**). In addition, the variability in Phe was significantly lower at all ages (**Table 2**).

PAH deficient patients not requiring treatment treatment had average lifetime Phe concentrations below 360 μmol/L (**Table 1**). Only two patients assigned to this group had recurrent Phe concentrations between 360 and 600 μmol/L, all others had Phe concentrations < 360 μmol/L in healthy state. The variability in Phe was significantly lower in PAH deficient patients not requiring treatment compared with those requiring treatment ($p < 0.05$ for all Phe indices).

Retinal Neuroaxonal Degeneration in the Late-Diagnosed PKU Patients

Global pRNFL thickness was significantly reduced in the late-diagnosed PKU patients compared with age and sex matched HCs (mean ± SD 88 ± 7.9 vs. 100 ± 6.4 μm) (**Figure 1A**).

Due to the intellectual disability, two of the patients showed poor persistence during the OCT examination. Thus, performing a complete macular scan was possible only in the remaining two patients. In them, the volume of GCIPL was reduced compared with HCs (mean ± SD 0.5 ± 0.1 vs. 0.63 ± 0.04 mm^3) (**Figure 1A**).

Retinal Neuroaxonal Degeneration in the ETPKU Patients

Spectral-domain OCT studies were performed in 39 adult and 31 pediatric ETPKU patients.

The adult ETPKU patients showed a significant reduction in GCIPL volume compared with HCs (mean ± SD 0.59 ± 0.04 vs. 0.61 ± 0.05 mm^3, $p = 0.035$). No significant differences were observed for the other macular layers and global pRNFL thickness (ETPKU vs. HCs: mean ± SD 100.1 ± 8.3 vs. 100.8 ± 8.7 μm, $p = 0.678$), even when only the temporal quadrant was considered (ETPKU vs. HCs: mean ± SD 70.6 ± 10.7 vs. 73.2 ± 15.5 μm, $p = 0.375$).

As a next step, data from BH_4 responsive and non-responsive ETPKU patients were analyzed separately. BH_4 non-responsive patients showed a significant reduction in GCIPL and IRL volume compared with HCs (**Table 3**). Again, no significant difference was observed for global and single quadrant pRNFL thickness. In BH_4 responsive ETPKU patients, no significant alterations in any of the axonal or neuronal retinal layers were found (**Table 3**). Of note, BH_4 non-responsive patients had significantly higher Phe levels and variations (**Table 2**).

To investigate whether the observed differences were connected to higher average Phe levels, we compared OCT parameters of the ETPKU1 and ETPKU2 patients to HCs. At this, the ETPKU2, but not ETPKU1 patients, showed a significantly reduced GCIPL volume compared with HCs (mean ± SD 0.58 ± 0.04 vs. 0.60 ± 0.05 mm^3) (**Figures 1B,C**). This finding was more pronounced, when analyzing the BH_4 non-responsive patients only (mean ± SD 0.56 ± 0.24 mm^3, $p = 0.003$).

Consistent with the reduced GCIPL volume, we also observed a significantly reduced IRL volume in the ETPKU2 cohort as compared with HCs (mean ± SD 1.58 ± 0.09

TABLE 2 | Phenylalanine indices of BH_4 responsive and non-responsive ETPKU patients.

	BH_4 responder ($N = 36$)		BH_4 non-responder ($N = 34$)		
	Mean	**SD**	**Mean**	**SD**	***p***
Blood Phe [μmol/l]					
Childhood (0–10 years)					
IDC	250	96	269	96	*0.431*
Average of yearly SD	131	43	182	50	*0.000**
Adolescence (11–16 years)					
IDC	429	182	565	214	*0.018**
Average of yearly SD	131	55	180	54	*0.002**
Adulthood (17 years +)					
IDC	551	253	780	332	*0.017**
Average of yearly SD	114	52	176	66	*0.002**
Lifetime					
IDC	331	144	482	244	*0.002**
Mean Phe	322	135	445	208	*0.004**
Average of yearly SD	122	37	180	39	*0.000**
SD Phe	194	94	307	84	*0.000**

*Abbreviations: IDC, average of yearly median phenylalanine levels; Phe, phenylalanine. *p < 0.05, p-values were calculated using the unpaired t-test.*

TABLE 3 | OCT findings related to phenotype of PAH deficient patients diagnosed within the neonatal period by newborn screening.

	HC		**PAH deficiency, not requiring treatment**			**PAH deficiency, requiring treatment**					
						BH_4 **responder**			BH_4 **non-responder**		
age ≥ 18 years	**(*N* = 49)**		**(*N* = 9)**			**(*N* = 20)**			**(*N* = 19)**		
	Mean	**SD**	**Mean**	**SD**	***p***	**Mean**	**SD**	***p***	**Mean**	**SD**	***p***
global pRNFL[μm]	100.83	8.70	103.83	5.18	*0.356*	101.57	8.53	*0.942*	98.47	8.02	*0.545*
TMV [mm^3]	2.16	0.11	2.14	0.08	*0.934*	2.15	0.11	*0.938*	2.10	0.08	*0.123*
GCIPL [mm^3]	0.61	0.05	0.60	0.04	*0.843*	0.60	0.05	*0.592*	0.58	0.03	*0.021**
IRL [mm^3]	1.64	0.09	1.62	0.08	*0.814*	1.63	0.10	*0.782*	1.59	0.07	*0.033**
age 6–17 years	**(*N* = 14)**		**(*N* = 9)**			**(*N* = 16)**			**(*N* = 15)**		
	Mean	**SD**	**Mean**	**SD**	***p***	**Mean**	**SD**	***p***	**Mean**	**SD**	***p***
global pRNFL [μm]	106.46	5.06	105.17	9.35	*0.923*	105.50	10.12	*0.940*	103.20	9.46	*0.483*
TMV [mm^3]	2.16	0.08	2.14	0.07	*0.905*	2.18	0.14	*0.919*	2.12	0.10	*0.610*
GCIPL [mm^3]	0.63	0.05	0.60	0.02	*0.280*	0.61	0.05	*0.663*	0.60	0.05	*0.233*
IRL [mm^3]	1.63	0.08	1.62	0.06	*0.892*	1.66	0.13	*0.815*	1.61	0.10	*0.787*

*pRNFL, peripapillary retinal nerve fiber layer; TMV, total macular volume; GCIPL, ganglion cell and inner plexiform layer; IRL, inner retinal layer; HC, healthy control; PAH, phenylalanine hydroxylase. *p < 0.05, comparison analysis was performed by Anova and Games-Howell post-hoc test, the p-values are given in comparison to age-matched HCs.*

vs. 1.64 ± 0.09 mm^3, $p = 0.007$). Although differences did not reach the level of significance (ETPKU2 vs. HCs: mean ± SD 2.1 ± 0.09 vs. 2.2 ± 0.11 mm^3, $p = 0.051$), we found TMV atrophy in individual patients as depicted in **Figure 1C**.

Again, there was no significant difference in global pRNFL thickness of ETPKU1 vs. ETPKU2 vs. HCs (mean ± SD 101 ± 8.4 vs. 99.3 ± 8.4 vs. 100.3 ± 8.1 μm) (**Figure 1B**). This was evident when considering all pRNFL sectors individually, as well as temporal pRNFL with the papillomacular bundle (PMD) (ETPKU1 vs. ETPKU2 vs. HCs: mean ± SD 72.7 ± 9.8 vs. 69.2 ± 11.2 vs. 73.2 ± 15.5 μm).

Analyzing the pediatric ETPKU patients revealed no significant difference in macular layers (mean ± SD; GCIPL 0.60

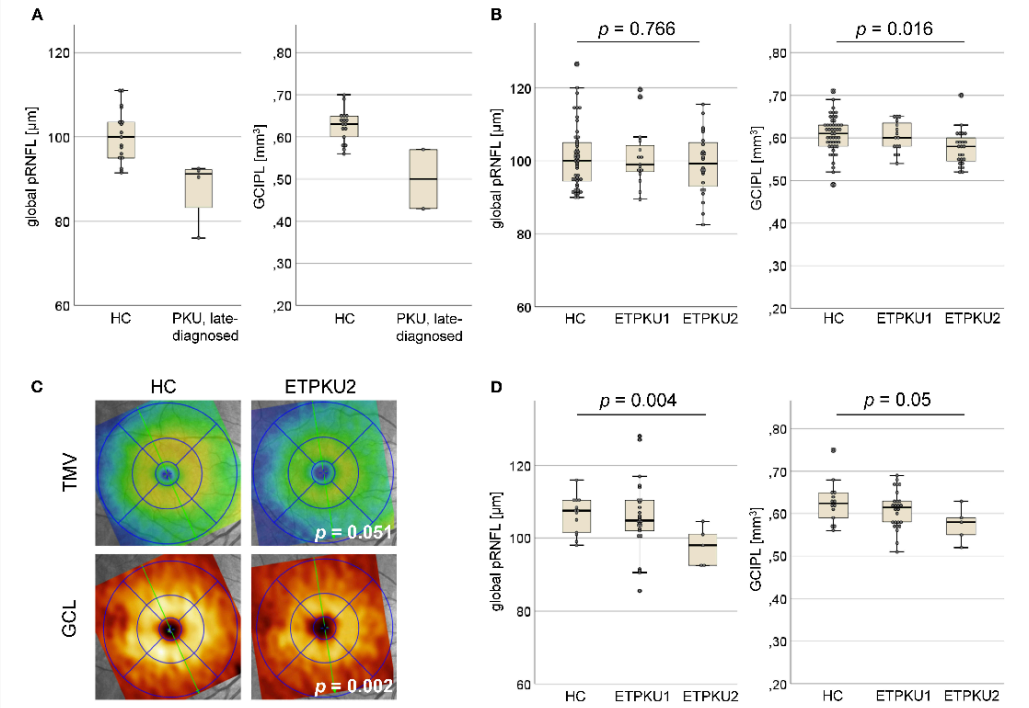

FIGURE 1 | Axonal and neuronal degeneration in phenylketonuria (PKU). **(A)** Global peripapillary retinal nerve fiber layer (pRNFL) thickness and ganglion cell and inner plexiform layer (GCIPL) volume in the late-diagnosed PKU patients compared with HCs ($N = 42$). **(B)** Global pRNFL thickness and GCIPL volume in early treated phenylketonuria (ETPKU) ≥ 18 years of age compared with HCs ($N = 49$). Based on average of yearly median phenylalanine levels (IDC) (as shown in **Table 1**) in childhood, adolescence, and adulthood, the metabolic control of patients was analyzed and ETPKU were grouped according to adherence to European Union (EU) guidelines (ETPKU1; IDC in childhood <360 and <600 µmol/L after that, $N = 15$, ETPKU2; IDC in childhood >360 µmol/L and/or >600 µmol/L after that, $N = 24$). **(C)** Total macular volume (TMV) and ganglion cell layer (GCL) volume in ETPKU2 ≥ 18 years of age. Depicted is the heat map of the examination of a single patient with ETPKU2 and the corresponding HC, with a coding for TMV (blue tones; low volume, yellow/red tones; high volume) and GCL (brown tones; low volume, yellow tones; high volume). **(D)** Global pRNFL thickness and GCIPL volume in HCs ($N = 14$), ETPKU1 ($N = 26$), and ETPKU2 ($N = 5$) from 6 to 17 years of age. The p-values are given for comparisons between the ETPKU2 cohort and HCs.

± 0.05 mm^3, TMV 2.14 ± 0.12 mm^3, IRL 1.63 ± 0.11 mm^3) and pRNFL thickness (mean ± SD 103 ± 10.0) as compared with HCs. Separate analysis for BH_4 responsiveness also revealed no differences (**Table 3**).

However, assigning pediatric ETPKU patients to the subgroups based on average Phe levels, a significantly reduced global pRNFL thickness was found in the ETPKU2 group in comparison with HCs (mean ± SD 98 ± 5.3 vs. 107 ± 5.1 µm; $p = 0.004$) (**Figure 1D**). In addition, there was a trend of GCIPL reduction in ETPKU2 patients (ETPKU2 vs. HCs: mean ± SD 0.57 ± 0.04 vs. 0.63 ± 0.05 mm^3) and it was notable that individual patients in the ETPKU1 group also had reduced pRNFL thicknesses and GCIPL volumes compared with the HC group (**Figure 1D**).

OCT in the PAH Deficient Patients Not Requiring Treatment

This group of patients did not show differences in any of the OCT parameters analyzed compared with HCs (**Table 3**). Of note, two of these patients had recurrent Phe values between 360 and 600 µmol/L but did not show retinal neuroaxonal degeneration (pRNFL; mean ± SD 105 ± 9.5 µm, GCIPL; mean ± SD 0.59 ± 0.03 mm^3).

Correlation Analyses of GCIPL Volume and Metabolic Indices

Looking at indices for Phe elevation, IDC in adulthood and lifetime, mean Phe and mean exposure was significantly negatively associated with GCIPL volume (**Figure 2A**). For IDC

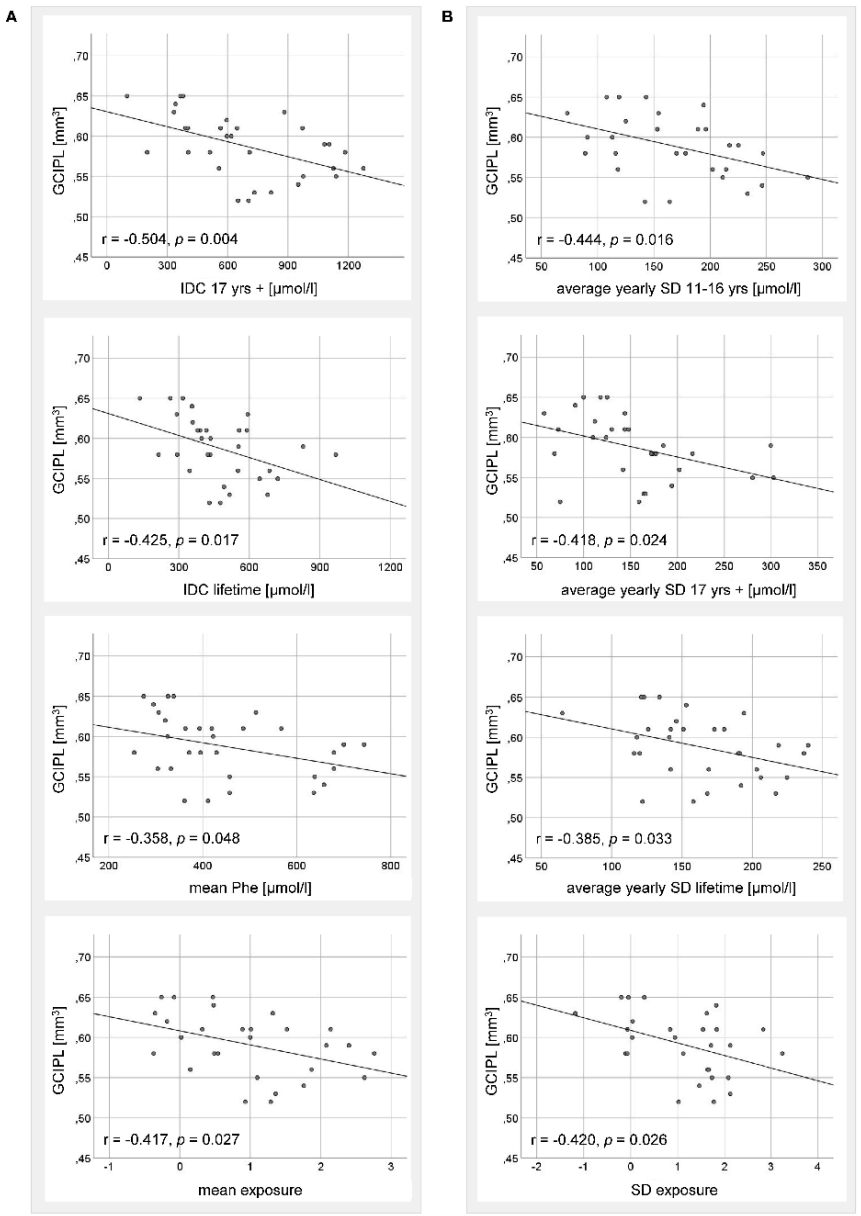

FIGURE 2 | Correlation analysis between GCIPL volume of adult ETPKU patients 18–33 years of age ($N = 32$) and metabolic indices for **(A)** Phe elevation, and **(B)** Phe variability. IDC; average of yearly median Phe levels. The Pearson *r*- and *p*-values are indicated. The relationship of the correlating variables was linear, as depicted by the continuous line.

in childhood ($r = 0.060$, $p = 0.753$) and adolescence ($r = -0.268$, $p = 0.152$), no significant correlations were found.

Looking at indices for Phe variation, average yearly SD in adolescence, adulthood, and lifetime, as well as SD exposure were significantly negatively associated with GCIPL volume (**Figure 2B**). The average yearly SD in childhood ($r = 0.026$, $p = 0.890$) and the SD Phe ($r = -0.347$, $p = 0.056$) showed no significant correlations.

Retinal Inner Nuclear Layer Volume in the ETPKU Patients

In adult ETPKU patients, no significant increase in INL volume compared with HCs was found (mean ± SD 0.25 ± 0.02 vs. 0.25 ± 0.02 mm^3, $p = 0.901$), not even when analyzing only patients with a current Phe level of >600 µmol/L (**Figure 3A**). In general, INL volume did not correlate with the current Phe level ($r = 0.12$, $p = 0.604$).

In pediatric ETPKU patients, INL volume was significantly higher compared with HCs (mean ± SD 0.26 ± 0.03 vs. 0.24 ± 0.01 mm^3, $p = 0.017$). This finding was more pronounced, when comparing only pediatric ETPKU patients with a current Phe level > 600 µmol/L to HCs (mean ± SD 0.27 ± 0.02 vs. 0.24 ± 0.01 mm^3) (**Figure 3B**). However, we observed increased INL volume in a few patients with a current Phe level <600 µmol/L (**Figure 3B**) and there was no overall correlation of INL volume with the current Phe level ($r = 0.109$, $p = 0.559$).

DISCUSSION

To evaluate the potential of OCT parameters as markers of neurodegeneration in PAH deficiency, we performed spectral-domain OCT in pediatric and adult patients covering the complete phenotypic spectrum of PAH deficiency. Our major findings were (i) evidence of retinal neuroaxonal degeneration in late-diagnosed PKU patients, (ii) retinal neuroaxonal degeneration of varying degree related to age and metabolic control in ETPKU patients, (iii) no evidence of retinal degeneration in PAH deficient patients not requiring treatment, and (iv) increased INL volume in pediatric ETPKU patients.

In severely affected PKU patients, WMLs, most likely reflecting a lack of myelin formation, have been described (17, 23, 53). Consistent with this, the severely affected, late-diagnosed patients in our cohort showed reduced GCIPL volume and pRNFL thickness, suggesting retinal neuronal and axonal degeneration, respectively. These findings support the hypothesis of OCT parameters being potential markers of neurodegeneration in PAH deficiency.

The patients with PAH deficiency in whom Phe concentrations are found to be <600 µmol/L without treatment throughout life, represent the mildest manifestation of PAH deficiency and, thus, the opposite end of the phenotypic spectrum. These patients have been described to show no WMLs (12). Consistent with these findings, PAH deficient patients not requiring treatment in our cohort did not show any signs of retinal neuroaxonal degeneration. Since the majority of our patients in this group had Phe concentrations <360 µmol/L,

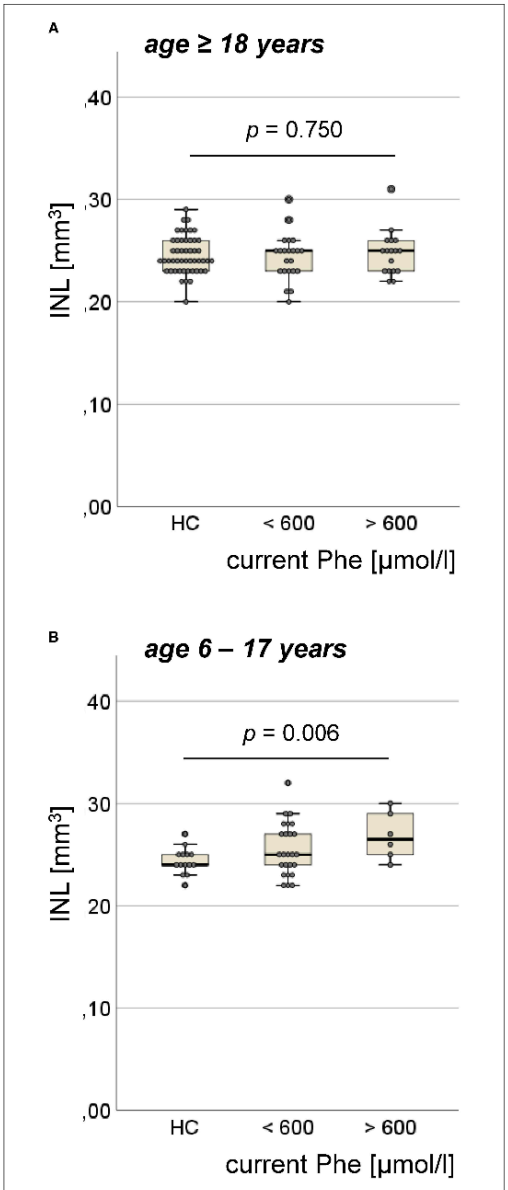

FIGURE 3 | Volume of inner nuclear layer (INL) in the ETPKU patients. **(A)** ETPKU ≥ 18 years of age with current Phe level < 600 µmol/L ($N = 22$) or >600 µmol/L ($N = 17$), and HCs ($N = 49$). **(B)** ETPKU 6–17 years of age with current Phe level <600 µmol/L ($N = 25$) or >600 µmol/L ($N = 6$), and HCs ($N = 14$). The *p*-values are given for comparison between ETPKU with current Phe level >600 µmol/L and HCs.

our data mainly confirm the approach of not treating patients with baseline Phe concentrations below < 360 μmol/L (2, 11). However, two of our patients had recurrent Phe levels between 360 and 600 μmol/L and did not show retinal neuroaxonal degeneration. With the limitation of two patients only, our data support the view of no indication for treatment in the patients with Phe concentrations below 600 μmol/L (12, 14). Of note, in both phenotypes, late-diagnosed PKU patients and PAH deficient patients not requiring treatment, the OCT studies have not been described so far.

In the ETPKU cohort, adult patients showed a significantly reduced GCIPL volume, indicating retinal neuronal degeneration. The observed effect was driven by the patients with poorer metabolic control, who also had a decreased IRL volume. This might also explain why BH_4 non-responsive patients but not BH_4 responsive patients showed significant neuronal degeneration. In patients who do not respond to BH_4, good metabolic control is more difficult to achieve (5). This was also reflected by the significantly higher mean Phe levels and variability in BH_4 non-responsive patients in our cohort. Accordingly, a correlation analysis demonstrated a negative association between GCIPL volume and indices of Phe elevation in adulthood or lifetime, and Phe variability from adolescence onward. Considering the good and consistent metabolic control of our adult cohort during childhood (IDC < 360 μmol/L), a correlation analysis of GCIPL volume and childhood Phe indices was not meaningful. Based on these data one might hypothesize that retinal neuronal degeneration in adult ETPKU patients is triggered by increased and highly fluctuating Phe levels, whereas patients with good metabolic control do not show signs of retinal neuronal degeneration. Our observation of retinal neuronal degeneration in ETPKU is in line with the recent study of Serfozo et al. demonstrating significant IRL thinning in ETPKU compared with HCs (39, 40). However, this study described correlations to be found solely between the parafoveal IRL thickness and Phe levels within the last 10 years and therefore concluded no overall correlation between ganglion cell complex layer thickness and metabolic control (40). The discrepancies to our correlation analysis may arise from the OCT parameters analyzed and different OCT protocols used. Based on the experience of other diseases, GCIPL has been shown to be a reliable and sensitive marker of neurodegeneration (28, 54, 55). We therefore propose GCIPL as a standard parameter to be included in future OCT studies in ETPKU. In contrast, Hopf et al. found no retinal alterations in a small cohort of ETPKU patients (37).

The reduction of GCIPL volume was significant for adults, but not for the pediatric cohort. The observation that neuronal damage increases with age is in line with a report from MRT studies demonstrating increased WMLs with age (56). Nevertheless, there was a trend toward lower GCIPL volume also in our pediatric patients with poorer metabolic control. The metabolic control in our pediatric cohort was, overall, very good. Only 5 out of 31 patients had average Phe values outside the European treatment recommendations. This small number might be one reason why the level of significance was not reached.

Assessing axonal degeneration, we did not observe reduced pRNFL thickness in the adult ETPKU patients, not even in the patients with poorer metabolic control. A reduced pRNFL thickness was also not observed when the temporal quadrant with the particularly vulnerable papillomacular bundles (57) was analyzed separately. This finding is conflicting with the study of Serfozo et al. reporting significantly reduced pRNFL thickness in adult ETPKU correlating with the blood Phe levels (39). In line with the study of Nowak et al. (38), however, we found a significantly reduced pRNFL thickness in pediatric ETPKU patients with average Phe concentrations outside the recommended range.

As expected from other similar indications (34, 35), the changes in OCT parameters reported by us and the other ETPKU studies were small (38–40). Taking into account that PAH deficiency is a rare disease and various factors (e.g., phenotype, metabolic control, and age) might have an impact on retinal neuroaxonal degeneration, a potential bias could be caused by the study-specific characteristics. A possible influence on OCT measures could also result from previously unrecognized ocular or systemic comorbidities. This could be particularly the case in the elderly study participants. However, the risk of influence was minimized by the exclusion criteria, especially since the bias affected both the PKU and HC cohorts. Nevertheless, larger studies are needed to minimize potential bias. OCT is well-suited for standardized data collection (58), enabling multicenter approaches for cross-sectional and longitudinal studies.

Whether the observed retinal changes relate to WML burden remains speculative as MRI scans were not available in any of the OCT studies (38–40), including ours. However, WMLs have repeatedly been described in ETPKU patients with the underlying molecular mechanisms remaining elusive (17–19, 59–63). Intramyelinic edema is primarily thought to be responsible for reversible WMLs (17), but impairment of microstructural development has also been described (59). Likewise, the pathophysiology underlying the described retinal neuroaxonal alterations is not yet understood. Serfozo et al. speculated that alterations in the dopamine levels might contribute to retinal degeneration in ETPKU (39, 40) as it has been suggested for other diseases with perturbations in the dopaminergic system, such as Parkinson's disease (64, 65). Dopamine plays a complex role in visual processing (66, 67), and dopaminergic cells are located mainly in the INL (66–69). An investigation of the INL in ETPKU has been suggested (40), but until now, no study has been available.

Our pediatric cohort showed an increased INL volume, and this effect was particularly influenced by those patients with high current Phe concentrations. In other disorders, INL swelling has been associated with macular edema (70) and/or inflammatory activity (71–74). The pathogenesis of INL swelling in our cohort is ultimately unclear. The INL contains a relevant number of Müller cells involved in retinal environmental homeostasis (75). They play a critical role in the regulation of extracellular space volume, water homeostasis, modulation of inflammatory responses, and contribute to oxidative stress (75, 76). It has been previously suggested, that elevated Phe concentrations can induce oxidative stress (77). Therefore, it could be hypothesized

that the increased Phe concentrations lead to oxidative stress that triggers activation of Müller glial cells, resulting in swelling of the INL either through Müller cell hypertrophy or edema. Whether neuroinflammatory processes, as repeatedly discussed in PKU (60), also play a role remains speculation.

In ETPKU, no WMLs have been described below Phe concentrations of 360 μmol/L, data at concentrations between 360 and 600 μmol/L are inconsistent (25, 78, 79). In our cohort, we saw individual ETPKU patients with Phe values <600 μmol/L who had increased INL volume, but there was no overall correlation of the INL volume with the current Phe level. Longitudinal studies are needed to show whether the increase in INL volume will be reversible with improved metabolic control, as has been shown for the WMLs (25, 26). In addition, it remains to be clarified why pediatric but not adult patients showed abnormalities of the INL. One might hypothesize that the developmental switch of retinal cells in the INL may play a role (80).

In conclusion, our data on spectral-domain OCT in PAH deficiency covering the full phenotypic spectrum of the disease provide evidence of retinal neuroaxonal degeneration and INL swelling depending on phenotype, current age, and metabolic control. These findings suggest that OCT is a suitable marker to investigate neurodegeneration in PKU. We propose OCT as a sensitive, reliable, safe, low-burden, and low-cost examination to contribute to the urgent questions of treatment indications and targets in future larger and multicenter studies.

DATA AVAILABILITY STATEMENT

The original contributions presented in the study are included in the article/supplementary material, further inquiries can be directed to the corresponding author/s.

ETHICS STATEMENT

The studies involving human participants were reviewed and approved by Ethics Committee of the Ludwig-Maximilians-University of Munich, Medical Faculty. Written informed consent to participate in this study was provided by the participant, and/or the participants' legal guardian/next of kin.

AUTHOR CONTRIBUTIONS

AL-H designed and conceptualized the study, played a major role in the acquisition of data, analyzed the data, was responsible for the statistical analyses, and drafted the manuscript. JH designed and conceptualized the study, played a major role in the acquisition of data, and drafted the manuscript. EM designed and conceptualized the study and drafted the manuscript. TC, LB, SR-V, KW, KS, and KP were involved in the acquisition of data. All the authors contributed to the final version of the manuscript.

FUNDING

This study was supported by a research grant from Nutricia Metabolics. JH is (partially) funded by the German Federal Ministry of Education and Research [Grant Numbers 01ZZ1603[A-D] and 01ZZ1804[A-H] (DIFUTURE)].

ACKNOWLEDGMENTS

We would like to thank Angelika Bamberger and Sabine Lüngen for their excellent technical support. We are grateful to the patients, healthy controls, and their families for their participation in this study.

REFERENCES

1. Blau N, van Spronsen FJ, Levy HL. Phenylketonuria. *Lancet.* (2010) 376:1417–27. doi: 10.1016/S0140-6736(10)60961-0
2. van Wegberg AMJ, MacDonald A, Ahring K, Belanger-Quintana A, Blau N, Bosch AM, et al. The complete European guidelines on phenylketonuria: diagnosis and treatment. *Orphanet J Rare Dis.* (2017) 12:162. doi: 10.1186/s13023-017-0685-2
3. Paine RS. The variability in manifestations of untreated patients with phenylketonuria (phenylpyruvic aciduria). *Pediatrics.* (1957) 20:290–302.
4. Enns GM, Koch R, Brumm V, Blakely E, Suter R, Jurecki E. Suboptimal outcomes in patients with PKU treated early with diet alone: revisiting the evidence. *Mol Genet Metab.* (2010) 101:99–109. doi: 10.1016/j.ymgme.2010.05.017
5. Keil S, Anjema K, van Spronsen FJ, Lambruschini N, Burlina A, Belanger-Quintana A, et al. Long-term follow-up and outcome of phenylketonuria patients on sapropterin: a retrospective study. *Pediatrics.* (2013) 131:e1881–8. doi: 10.1542/peds.2012-3291
6. Muntau AC, Burlina A, Eyskens F, Freisinger P, De Laet C, Leuzzi V, et al. Efficacy, safety and population pharmacokinetics of sapropterin in PKU patients <4 years: results from the SPARK open-label, multicentre, randomized phase IIIb trial. *Orphanet J Rare Dis.* (2017) 12:47. doi: 10.1186/s13023-017-0600-x
7. Muntau AC, Roschinger W, Habich M, Demmelmair H, Hoffmann B, Sommerhoff CP, et al. Tetrahydrobiopterin as an alternative treatment for mild phenylketonuria. *N Engl J Med.* (2002) 347:2122–32. doi: 10.1056/NEJMoa021654
8. Longo N, Dimmock D, Levy H, Viau K, Bausell H, Bilder DA, et al. Evidence- and consensus-based recommendations for the use of pegvaliase in adults with phenylketonuria. *Genet Med.* (2019) 21:1851–67. doi: 10.1038/s41436-018-0403-z
9. Thomas J, Levy H, Amato S, Vockley J, Zori R, Dimmock D, et al. Pegvaliase for the treatment of phenylketonuria: results of a long-term phase 3 clinical trial program (PRISM). *Mol Genet Metab.* (2018) 124:27–38. doi: 10.1016/j.ymgme.2018.03.006
10. Vockley J, Andersson HC, Antshel KM, Braverman NE, Burton BK, Frazier DM, et al. Phenylalanine hydroxylase deficiency: diagnosis and management guideline. *Genet Med.* (2014) 16:188–200. doi: 10.1038/gim.2013.157
11. Gassio R, Artuch R, Vilaseca MA, Fuste E, Boix C, Sans A, et al. Cognitive functions in classic phenylketonuria and mild hyperphenylalaninaemia: experience in a paediatric population. *Dev Med Child Neurol.* (2005) 47:443–8. doi: 10.1017/S0012162205000861
12. Weglage J, Pietsch M, Feldmann R, Koch HG, Zschocke J, Hoffmann G, et al. Normal clinical outcome in untreated subjects with mild hyperphenylalaninemia. *Pediatr Res.* (2001) 49:532–6. doi: 10.1203/00006450-200104000-00015
13. Costello PM, Beasley MG, Tillotson SL, Smith I. Intelligence in mild atypical phenylketonuria. *Eur J Pediatr.* (1994) 153:260–3. doi: 10.1007/BF01954515
14. Smith ML, Saltzman J, Klim P, Hanley WB, Feigenbaum A, Clarke JT. Neuropsychological function in mild

hyperphenylalaninemia. *Am J Ment Retard.* (2000) 105:69–80. doi: 10.1352/0895-8017(2000)105<0069:NFIMH>2.0.CO;2
15. Campistol J, Gassio R, Artuch R, Vilaseca MA. Unit PKUF-u. Neurocognitive function in mild hyperphenylalaninemia. *Dev Med Child Neurol.* (2011) 53:405–8. doi: 10.1111/j.1469-8749.2010.03869.x
16. van Spronsen FJ. Mild hyperphenylalaninemia: to treat or not to treat. *J Inherit Metab Dis.* (2011) 34:651–6. doi: 10.1007/s10545-011-9283-y
17. Anderson PJ, Leuzzi V. White matter pathology in phenylketonuria. *Mol Genet Metab.* (2010) 99:S3–9. doi: 10.1016/j.ymgme.2009.10.005
18. Hawks Z, Hood AM, Lerman-Sinkoff DB, Shimony JS, Rutlin J, Lagoni D, et al. White and gray matter brain development in children and young adults with phenylketonuria. *Neuroimage Clin.* (2019) 23:101916. doi: 10.1016/j.nicl.2019.101916
19. Hood A, Antenor-Dorsey JA, Rutlin J, Hershey T, Shimony JS, McKinstry RC, et al. Prolonged exposure to high and variable phenylalanine levels over the lifetime predicts brain white matter integrity in children with phenylketonuria. *Mol Genet Metab.* (2015) 114:19–24. doi: 10.1016/j.ymgme.2014.11.007
20. Antenor-Dorsey JA, Hershey T, Rutlin J, Shimony JS, McKinstry RC, Grange DK, et al. White matter integrity and executive abilities in individuals with phenylketonuria. *Mol Genet Metab.* (2013) 109:125–31. doi: 10.1016/j.ymgme.2013.03.020
21. Peng H, Peck D, White DA, Christ SE. Tract-based evaluation of white matter damage in individuals with early-treated phenylketonuria. *J Inherit Metab Dis.* (2014) 37:237–43. doi: 10.1007/s10545-013-9650-y
22. White DA, Connor LT, Nardos B, Shimony JS, Archer R, Snyder AZ, et al. Age-related decline in the microstructural integrity of white matter in children with early- and continuously-treated PKU: a DTI study of the corpus callosum. *Mol Genet Metab.* (2010) 99:S41–6. doi: 10.1016/j.ymgme.2009.09.016
23. Leuzzi V, Tosetti M, Montanaro D, Carducci C, Artiola C, Carducci C, et al. The pathogenesis of the white matter abnormalities in phenylketonuria. A multimodal 30 tesla MRI and magnetic resonance spectroscopy (1H MRS) study. *J Inherit Metab Dis.* (2007) 30:209–16. doi: 10.1007/s10545-006-0399-4
24. Thompson AJ, Tillotson S, Smith I, Kendall B, Moore SG, Brenton DP. Brain MRI changes in phenylketonuria. Associations with dietary status. *Brain.* (1993) 116:811–21. doi: 10.1093/brain/116.4.811
25. Bick U, Ullrich K, Stober U, Moller H, Schuierer G, Ludolph AC, et al. White matter abnormalities in patients with treated hyperphenylalaninaemia: magnetic resonance relaxometry and proton spectroscopy findings. *Eur J Pediatr.* (1993) 152:1012–20. doi: 10.1007/BF01957228
26. Cleary MA, Walter JH, Wraith JE, White F, Tyler K, Jenkins JP. Magnetic resonance imaging in phenylketonuria: reversal of cerebral white matter change. *J Pediatr.* (1995) 127:251–5. doi: 10.1016/S0022-3476(95)70303-9
27. Galetta KM, Calabresi PA, Frohman EM, Balcer LJ. Optical coherence tomography (OCT): imaging the visual pathway as a model for neurodegeneration. *Neurotherapeutics.* (2011) 8:117–32. doi: 10.1007/s13311-010-0005-1
28. Petzold A, Balcer LJ, Calabresi PA, Costello F, Frohman TC, Frohman EM, et al. Retinal layer segmentation in multiple sclerosis: a systematic review and meta-analysis. *Lancet Neurol.* (2017) 16:797–812. doi: 10.1016/S1474-4422(17)30278-8
29. Oertel FC, Outteryck O, Knier B, Zimmermann H, Borisow N, Bellmann-Strobl J, et al. Optical coherence tomography in myelin-oligodendrocyte-glycoprotein antibody-seropositive patients: a longitudinal study. *J Neuroinflammation.* (2019) 16:154. doi: 10.1186/s12974-019-1521-5
30. Oertel FC, Havla J, Roca-Fernandez A, Lizak N, Zimmermann H, Motamedi S, et al. Retinal ganglion cell loss in neuromyelitis optica: a longitudinal study. *J Neurol Neurosurg Psychiatry.* (2018) 89:1259–65. doi: 10.1136/jnnp-2018-318382
31. Filippatou AG, Mukharesh L, Saidha S, Calabresi PA, Sotirchos ES. AQP4-IgG and MOG-IgG related optic neuritis-prevalence, optical coherence tomography findings, and visual outcomes: a systematic review and meta-analysis. *Front Neurol.* (2020) 11:540156. doi: 10.3389/fneur.2020.540156
32. Albrecht P, Muller AK, Sudmeyer M, Ferrea S, Ringelstein M, Cohn E, et al. Optical coherence tomography in parkinsonian syndromes. *PLoS ONE.* (2012) 7:e34891. doi: 10.1371/journal.pone.0034891
33. Cunha LP, Almeida AL, Costa-Cunha LV, Costa CF, Monteiro ML. The role of optical coherence tomography in Alzheimer's disease. *Int J Retina Vitreous.* (2016) 2:24. doi: 10.1186/s40942-016-0049-4
34. Albrecht P, Muller AK, Ringelstein M, Finis D, Geerling G, Cohn E, et al. Retinal neurodegeneration in Wilson's disease revealed by spectral domain optical coherence tomography. *PLoS ONE.* (2012) 7:e49825. doi: 10.1371/journal.pone.0049825
35. Havla J, Moser M, Sztatecsny C, Lotz-Havla AS, Maier EM, Hizli B, et al. Retinal axonal degeneration in Niemann-Pick type C disease. *J Neurol.* (2020) 267:2070–82. doi: 10.1007/s00415-020-09796-2
36. Hopf S, Hennermann JB, Schuster AK, Pfeiffer N, Pitz S. Vertical saccadic palsy and foveal retinal thinning in Niemann-Pick disease type C. *PLoS ONE.* (2021) 16:e0252825. doi: 10.1371/journal.pone.0252825
37. Hopf S, Nowak C, Hennermann JB, Schmidtmann I, Pfeiffer N, Pitz S. Saccadic reaction time and ocular findings in phenylketonuria. *Orphanet J Rare Dis.* (2020) 15:124. doi: 10.1186/s13023-020-01407-7
38. Nowak JK, Kaluzny L, Suda W, Bukowska-Posadzy A, Adams A, Grulkowski I, et al. Retinal nerve fibre layer thickness associates with phenylketonuria control and cognition. *J Med Genet.* (2020) 57:863–4. doi: 10.1136/jmedgenet-2019-106770
39. Serfozo C, Barta AG, Horvath E, Sumanszki C, Csakany B, Resch M, et al. Altered visual functions, macular ganglion cell and papillary retinal nerve fiber layer thickness in early-treated adult PKU patients. *Mol Genet Metab Rep.* (2020) 25:100649. doi: 10.1016/j.ymgmr.2020.100649
40. Serfozo C, Barta AG, Horvath E, Sumanszki C, Csakany B, Resch M, et al. Reduced macular thickness and macular vessel density in early-treated adult patients with PKU. *Mol Genet Metab Rep.* (2021) 27:100767. doi: 10.1016/j.ymgmr.2021.100767
41. van Dijk HW, Verbraak FD, Kok PH, Garvin MK, Sonka M, Lee K, et al. Decreased retinal ganglion cell layer thickness in patients with type 1 diabetes. *Invest Ophthalmol Vis Sci.* (2010) 51:3660–5. doi: 10.1167/iovs.09-5041
42. van Dijk HW, Verbraak FD, Kok PH, Stehouwer M, Garvin MK, Sonka M, et al. Early neurodegeneration in the retina of type 2 diabetic patients. *Invest Ophthalmol Vis Sci.* (2012) 53:2715–9. doi: 10.1167/iovs.11-8997
43. Tong AY, El-Dairi M, Maldonado RS, Rothman AL, Yuan EL, Stinnett SS, et al. Evaluation of optic nerve development in preterm and term infants using handheld spectral-domain optical coherence tomography. *Ophthalmology.* (2014) 121:1818–26. doi: 10.1016/j.ophtha.2014.03.020
44. Demir M, Oba E, Can E, Odabasi M, Tiryaki S, Ozdal E, et al. Foveal and parafoveal retinal thickness in healthy pregnant women in their last trimester. *Clin Ophthalmol.* (2011) 5:1397–400. doi: 10.2147/OPTH.S23944
45. Blau N, Hennermann JB, Langenbeck U, Lichter-Konecki U. Diagnosis, classification, and genetics of phenylketonuria and tetrahydrobiopterin (BH4) deficiencies. *Mol Genet Metab.* (2011) 104:S2–9. doi: 10.1016/j.ymgme.2011.08.017
46. Burgard P, Bremer HJ, Buhrdel P, Clemens PC, Monch E, Przyrembel H, et al. Rationale for the German recommendations for phenylalanine level control in phenylketonuria 1997. *Eur J Pediatr.* (1999) 158:46–54. doi: 10.1007/s004310051008
47. Schippling S, Balk LJ, Costello F, Albrecht P, Balcer L, Calabresi PA, et al. Quality control for retinal OCT in multiple sclerosis: validation of the OSCAR-IB criteria. *Multiple Sclerosis.* (2015) 21:163–70. doi: 10.1177/1352458514538110
48. Cruz-Herranz A, Balk LJ, Oberwahrenbrock T, Saidha S, Martinez-Lapiscina EH, Lagreze WA, et al. The APOSTEL recommendations for reporting quantitative optical coherence tomography studies. *Neurology.* (2016) 86:2303–9. doi: 10.1212/WNL.0000000000002774
49. Aytulun A, Cruz-Herranz A, Aktas O, Balcer LJ, Balk L, Barboni P. et al. The APOSTEL 20 recommendations for reporting quantitative optical coherence tomography studies. *Neurology.* (2021) 97:68–79. doi: 10.1212/WNL.0000000000012125
50. Romani C, Manti F, Nardecchia F, Valentini F, Fallarino N, Carducci C, et al. Adult cognitive outcomes in phenylketonuria: explaining causes of variability beyond average Phe levels. *Orphanet J Rare Dis.* (2019) 14:273. doi: 10.1186/s13023-019-1225-z
51. Hood A, Grange DK, Christ SE, Steiner R, White DA. Variability in phenylalanine control predicts IQ and executive abilities

in children with phenylketonuria. *Mol Genet Metab.* (2014) 111:445–51. doi: 10.1016/j.ymgme.2014.01.012
52. Meyer J, Karri R, Danesh-Meyer H, Drummond K, Symons A, A. Normative database of A-scan data using the heidelberg spectralis 4 spectral domain optical coherence tomography machine. *PLoS ONE.* (2021) 16:e0253720. doi: 10.1371/journal.pone.0253720
53. Leuzzi V, Trasimeni G, Gualdi GF, Antonozzi I. Biochemical, clinical and neuroradiological (MRI) correlations in late-detected PKU patients. *J Inherit Metab Dis.* (1995) 18:624–34. doi: 10.1007/BF02436009
54. Choi SH, Park SJ, Kim NR. Macular ganglion cell -inner plexiform layer thickness is associated with clinical progression in mild cognitive impairment and Alzheimers disease. *PLoS ONE.* (2016) 11:e0162202. doi: 10.1371/journal.pone.0162202
55. Cheung CY, Ong YT, Hilal S, Ikram MK, Low S, Ong YL, et al. Retinal ganglion cell analysis using high-definition optical coherence tomography in patients with mild cognitive impairment and Alzheimer's disease. *J Alzheimers Dis.* (2015) 45:45–56. doi: 10.3233/JAD-141659
56. Gonzalez MJ, Polo MR, Ripolles P, Gassio R, Ormazabal A, Sierra C, et al. White matter microstructural damage in early treated phenylketonuric patients. *Orphanet J Rare Dis.* (2018) 13:188. doi: 10.1186/s13023-018-0912-5
57. Petzold A, Nijland PG, Balk LJ, Amorini AM, Lazzarino G, Wattjes MP, et al. Visual pathway neurodegeneration winged by mitochondrial dysfunction. *Ann Clin Transl Neurol.* (2015) 2:140–50. doi: 10.1002/acn3.157
58. Oberwahrenbrock T, Traber GL, Lukas S, Gabilondo I, Nolan R, Songster C, et al. Multicenter reliability of semiautomatic retinal layer segmentation using OCT. *Neurol Neuroimmunol Neuroinflamm.* (2018) 5:e449. doi: 10.1212/NXI.0000000000000449
59. Wesonga E, Shimony JS, Rutlin J, Grange DK, White DA. Relationship between age and white matter integrity in children with phenylketonuria. *Mol Genet Metab Rep.* (2016) 7:45–9. doi: 10.1016/j.ymgmr.2016.03.003
60. Ferreira BK, Rodrigues MT, Streck EL, Ferreira GC, Schuck PF. White matter disturbances in phenylketonuria: possible underlying mechanisms. *J Neurosci Res.* (2021) 99:349–60. doi: 10.1002/jnr.24598
61. Leuzzi V, Gualdi GF, Fabbrizi F, Trasimeni G, Di Biasi C, Antonozzi I. Neuroradiological (MRI) abnormalities in phenylketonuric subjects: clinical and biochemical correlations. *Neuropediatrics.* (1993) 24:302–6. doi: 10.1055/s-2008-1071561
62. Mastrangelo M, Chiarotti F, Berillo L, Caputi C, Carducci C, Di Biasi C, et al. The outcome of white matter abnormalities in early treated phenylketonuric patients: a retrospective longitudinal long-term study. *Mol Genet Metab.* (2015) 116:171–7. doi: 10.1016/j.ymgme.2015.08.005
63. Nardecchia F, Manti F, Chiarotti F, Carducci C, Carducci C, Leuzzi V. Neurocognitive and neuroimaging outcome of early treated young adult PKU patients: a longitudinal study. *Mol Genet Metab.* (2015) 115:84–90. doi: 10.1016/j.ymgme.2015.04.003
64. Djamgoz MB, Hankins MW, Hirano J, Archer SN. Neurobiology of retinal dopamine in relation to degenerative states of the tissue. *Vision Res.* (1997) 37:3509–29. doi: 10.1016/S0042-6989(97)00129-6
65. Hajee ME, March WF, Lazzaro DR, Wolintz AH, Shrier EM, Glazman S, et al. Inner retinal layer thinning in Parkinson disease. *Arch Ophthalmol.* (2009) 127:737–41. doi: 10.1001/archophthalmol.2009.106
66. Witkovsky P. Dopamine and retinal function. *Doc Ophthalmol.* (2004) 108:17–40. doi: 10.1023/B:DOOP.0000019487.88486.0a
67. Indrieri A, Pizzarelli R, Franco B, De Leonibus E. Dopamine, alpha-synuclein, and mitochondrial dysfunctions in Parkinsonian eyes. *Front Neurosci.* (2020) 14:567129. doi: 10.3389/fnins.2020.567129
68. Frederick JM, Rayborn ME, Laties AM, Lam DM, Hollyfield JG. Dopaminergic neurons in the human retina. *J Comp Neurol.* (1982) 210:65–79. doi: 10.1002/cne.902100108
69. Dowling JE, Ehinger B. The interplexiform cell system. I Synapses of the dopaminergic neurons of the goldfish retina. *Proc R Soc Lond B Biol Sci.* (1978) 201:7–26. doi: 10.1098/rspb.1978.0030
70. Cunha-Vaz J, Santos T, Ribeiro L, Alves D, Marques I, Goldberg M. OCT-Leakage: a new method to identify and locate abnormal fluid accumulation in diabetic retinal edema. *Invest Ophthalmol Vis Sci.* (2016) 57:6776–83. doi: 10.1167/iovs.16-19999
71. Balk LJ, Coric D, Knier B, Zimmermann HG, Behbehani R, Alroughani R, et al. Retinal inner nuclear layer volume reflects inflammatory disease activity in multiple sclerosis; a longitudinal OCT study. *Mult Scler J Exp Transl Clin.* (2019) 5:2055217319871582. doi: 10.1177/2055217319871582
72. Cellerino M, Cordano C, Boffa G, Bommarito G, Petracca M, Sbragia E, et al. Relationship between retinal inner nuclear layer, age, and disease activity in progressive MS. *Neurol Neuroimmunol Neuroinflamm.* (2019) 6:e596. doi: 10.1212/NXI.0000000000000596
73. Saidha S, Sotirchos ES, Ibrahim MA, Crainiceanu CM, Gelfand JM, Sepah YJ, et al. Microcystic macular oedema, thickness of the inner nuclear layer of the retina, and disease characteristics in multiple sclerosis: a retrospective study. *Lancet Neurol.* (2012) 11:963–72. doi: 10.1016/S1474-4422(12)70213-2
74. Knier B, Schmidt P, Aly L, Buck D, Berthele A, Muhlau M, et al. Retinal inner nuclear layer volume reflects response to immunotherapy in multiple sclerosis. *Brain.* (2016) 139:2855–63. doi: 10.1093/brain/aww219
75. Bringmann A, Wiedemann P. Muller glial cells in retinal disease. *Ophthalmologica.* (2012) 227:1–19. doi: 10.1159/000328979
76. Bringmann A, Pannicke T, Grosche J, Francke M, Wiedemann P, Skatchkov SN, et al. Muller cells in the healthy and diseased retina. *Prog Retin Eye Res.* (2006) 25:397–424. doi: 10.1016/j.preteyeres.2006.05.003
77. Preissler T, Bristot IJ, Costa BM, Fernandes EK, Rieger E, Bortoluzzi VT, et al. Phenylalanine induces oxidative stress and decreases the viability of rat astrocytes: possible relevance for the pathophysiology of neurodegeneration in phenylketonuria. *Metab Brain Dis.* (2016) 31:529–37. doi: 10.1007/s11011-015-9763-0
78. Kono K, Okano Y, Nakayama K, Hase Y, Minamikawa S, Ozawa N, et al. Diffusion-weighted MR imaging in patients with phenylketonuria: relationship between serum phenylalanine levels and ADC values in cerebral white matter. *Radiology.* (2005) 236:630–6. doi: 10.1148/radiol.2362040611
79. Lou HC, Toft PB, Andresen J, Mikkelsen I, Olsen B, Guttler F, et al. An occipito-temporal syndrome in adolescents with optimally controlled hyperphenylalaninaemia. *J Inherit Metab Dis.* (1992) 15:687–95. doi: 10.1007/BF01800008
80. Bosco A, Cusato K, Nicchia GP, Frigeri A. Spray DC. A developmental switch in the expression of aquaporin-4 and Kir41 from horizontal to Muller cells in mouse retina. *Invest Ophthalmol Vis Sci.* (2005) 46:3869–75. doi: 10.1167/iovs.05-0385

Conflict of Interest: The authors declare that this study received funding from Nutritia Metabolics. The funder was not involved in the study design, collection, analysis, interpretation of data, the writing of this article or the decision to submit it for publication. AL-H has received travel reimbursement from BioMarin and Sobi. KW has received travel reimbursement from Sobi and Amicus Therapeutics, and honoraria for lectures from Sobi and Nutritia Metabolic. KS has received travel reimbursement from Shire and BioMarin. KP has received research funding and/or honoraria for consultancy and/or speaker's bureau activity from BioMarin, Sobi, Dr. Schaer. JH reports a grant for OCT research from the Friedrich-Baur-Stiftung, personal fees, and non-financial support from Merck, Alexion, Novartis, Roche, Santhera, Biogen, Heidelberg Engineering, Sanofi Genzyme, and non-financial support of the Guthy-Jackson Charitable Foundation, all outside the submitted work. EM has received travel reimbursement from Sobi and Dr. Schär and was paid for advisory services from Sobi, APR, and Sanofi-Aventis.

The remaining authors declare that the research was conducted in the absence of any commercial or financial relationships that could be construed as a potential conflict of interest.

Publisher's Note: All claims expressed in this article are solely those of the authors and do not necessarily represent those of their affiliated organizations, or those of the publisher, the editors and the reviewers. Any product that may be evaluated in this article, or claim that may be made by its manufacturer, is not guaranteed or endorsed by the publisher.

9. Literaturverzeichnis

1. Kuhlmann, T., et al., *Multiple sclerosis progression: time for a new mechanism-driven framework.* Lancet Neurol, 2023. **22**(1): p. 78-88.
2. Ontaneda, D., R.J. Fox, and J. Chataway, *Clinical trials in progressive multiple sclerosis: lessons learned and future perspectives.* Lancet Neurol, 2015. **14**(2): p. 208-23.
3. Deisenhammer, F., et al., *The Cerebrospinal Fluid in Multiple Sclerosis.* Front Immunol, 2019. **10**: p. 726.
4. Kolb, H., et al., *From pathology to MRI and back: Clinically relevant biomarkers of multiple sclerosis lesions.* Neuroimage Clin, 2022. **36**: p. 103194.
5. Gordon-Lipkin, E. and P.A. Calabresi, *Optical coherence tomography: A quantitative tool to measure neurodegeneration and facilitate testing of novel treatments for tissue protection in multiple sclerosis.* J Neuroimmunol, 2017. **304**: p. 93-96.
6. Ertl-Wagner, B., *Pädiatrische Neuroradiologie*. 2007, Berlin ; New York: Springer. xvii, 382 p.
7. Rohen, J.W. and E. Lütjen-Drecoll, *Funktionelle Embryologie: die Entwicklung der Funktionssysteme des menschlichen Organismus ; mit 9 Tabellen*. 2006: Schattauer.
8. Abalo-Lojo, J.M., et al., *Longitudinal study of retinal nerve fiber layer thickness changes in a multiple sclerosis patients cohort: A long term 5 year follow-up.* Mult Scler Relat Disord, 2018. **19**: p. 124-128.
9. Petzold, A., et al., *Diagnosis and classification of optic neuritis.* Lancet Neurol, 2022. **21**(12): p. 1120-1134.
10. Petzold, A., et al., *Retinal layer segmentation in multiple sclerosis: a systematic review and meta-analysis.* Lancet Neurol, 2017. **16**(10): p. 797-812.
11. Alonso, R., D. Gonzalez-Moron, and O. Garcea, *Optical coherence tomography as a biomarker of neurodegeneration in multiple sclerosis: A review.* Mult Scler Relat Disord, 2018. **22**: p. 77-82.
12. Huang, D., et al., *Optical coherence tomography.* Science, 1991. **254**(5035): p. 1178-81.
13. Forte, R., et al., *Comparison of time domain Stratus OCT and spectral domain SLO/OCT for assessment of macular thickness and volume.* Eye (Lond), 2009. **23**(11): p. 2071-8.
14. Aytulun, A., et al., *APOSTEL 2.0 Recommendations for Reporting Quantitative Optical Coherence Tomography Studies.* Neurology, 2021. **97**(2): p. 68-79.
15. Sotirchos, E.S., et al., *Progressive Multiple Sclerosis Is Associated with Faster and Specific Retinal Layer Atrophy.* Ann Neurol, 2020. **87**(6): p. 885-896.
16. Martinez-Lapiscina, E.H., et al., *Retinal thickness measured with optical coherence tomography and risk of disability worsening in multiple sclerosis: a cohort study.* Lancet Neurol, 2016. **15**(6): p. 574-84.
17. Balk, L.J., et al., *Retinal inner nuclear layer volume reflects inflammatory disease activity in multiple sclerosis; a longitudinal OCT study.* Mult Scler J Exp Transl Clin, 2019. **5**(3): p. 2055217319871582.
18. Knier, B., et al., *Retinal inner nuclear layer volume reflects response to immunotherapy in multiple sclerosis.* Brain, 2016. **139**(11): p. 2855-2863.
19. Havla, J., et al., *Interdisciplinary Risk Management in the Treatment of Multiple Sclerosis.* Dtsch Arztebl Int, 2016. **113**(51-52): p. 879-886.
20. Korsukewitz C, M.M., Wiendl H. , *MS-Versorgung heute und Vision für die Zukunft - eine Rolle für die ASV? .* NeuroTransmitter, 2022. **33(12):**: p. 32–7.
21. Schmidt, R.M., et al., *Multiple Sklerose*. 2021: Elsevier Health Sciences.

22. Doshi, A. and J. Chataway, *Multiple sclerosis, a treatable disease.* Clin Med (Lond), 2016. **16**(Suppl 6): p. s53-s59.
23. Kingwell, E., et al., *Incidence and prevalence of multiple sclerosis in Europe: a systematic review.* BMC Neurol, 2013. **13**: p. 128.
24. Thompson, A.J., et al., *Multiple sclerosis.* Lancet, 2018. **391**(10130): p. 1622-1636.
25. Jakimovski, D., et al., *Multiple sclerosis.* Lancet, 2024. **403**(10422): p. 183-202.
26. Belbasis, L., et al., *Environmental risk factors and multiple sclerosis: an umbrella review of systematic reviews and meta-analyses.* Lancet Neurol, 2015. **14**(3): p. 263-73.
27. Bjornevik, K., et al., *Longitudinal analysis reveals high prevalence of Epstein-Barr virus associated with multiple sclerosis.* Science, 2022. **375**(6578): p. 296-301.
28. Saidha, S., et al., *Primary retinal pathology in multiple sclerosis as detected by optical coherence tomography.* Brain, 2011. **134**(Pt 2): p. 518-33.
29. Dobson, R. and G. Giovannoni, *Multiple sclerosis - a review.* Eur J Neurol, 2019. **26**(1): p. 27-40.
30. Lublin, F.D., et al., *How patients with multiple sclerosis acquire disability.* Brain, 2022. **145**(9): p. 3147-3161.
31. (DGN), D.G.f.N., *Diagnose und Therapie der Multiplen Sklerose, Neuromyelitis-optica-Spektrum-Erkrankungen und MOG-IgG-assoziierten Erkrankungen.* 2023. **2. Aktualisierung als Living Guideline 2023**.
32. Albrecht, P., et al., *Optical coherence tomography measures axonal loss in multiple sclerosis independently of optic neuritis.* J Neurol, 2007. **254**(11): p. 1595-6.
33. Cree, B.A.C., et al., *Secondary Progressive Multiple Sclerosis: New Insights.* Neurology, 2021. **97**(8): p. 378-388.
34. Oh, J., et al., *Diagnosis and management of secondary-progressive multiple sclerosis: time for change.* Neurodegener Dis Manag, 2019. **9**(6): p. 301-317.
35. Plantone, D., et al., *Secondary Progressive Multiple Sclerosis: Definition and Measurement.* CNS Drugs, 2016. **30**(6): p. 517-26.
36. Miller, D.H. and S.M. Leary, *Primary-progressive multiple sclerosis.* Lancet Neurol, 2007. **6**(10): p. 903-12.
37. Travers, B.S., B.K. Tsang, and J.L. Barton, *Multiple sclerosis: Diagnosis, disease-modifying therapy and prognosis.* Aust J Gen Pract, 2022. **51**(4): p. 199-206.
38. Brownlee, W.J., et al., *Earlier and more frequent diagnosis of multiple sclerosis using the McDonald criteria.* J Neurol Neurosurg Psychiatry, 2015. **86**(5): p. 584-5.
39. Thompson, A.J., et al., *Diagnosis of multiple sclerosis: 2017 revisions of the McDonald criteria.* Lancet Neurol, 2018. **17**(2): p. 162-173.
40. Limmroth, V. and E. Sindern, *Multiple Sklerose*. 2004: Thieme.
41. Zheng, Y., et al., *Application of the 2017 McDonald criteria in a Chinese population with clinically isolated syndrome.* Ther Adv Neurol Disord, 2020. **13**: p. 1756286419898083.
42. Lublin, F.D., et al., *Defining the clinical course of multiple sclerosis: the 2013 revisions.* Neurology, 2014. **83**(3): p. 278-86.
43. Lebrun-Frenay, C., et al., *Radiologically isolated syndrome.* Lancet Neurol, 2023. **22**(11): p. 1075-1086.
44. Esmael, A., et al., *Retinal thickness as a potential biomarker of neurodegeneration and a predictor of early cognitive impairment in patients with multiple sclerosis.* Neurol Res, 2020. **42**(7): p. 564-574.
45. Cortese, R., et al., *Differentiating Multiple Sclerosis From AQP4-Neuromyelitis Optica Spectrum Disorder and MOG-Antibody Disease With Imaging.* Neurology, 2023. **100**(3): p. e308-e323.

46. Guerrieri, S., G. Comi, and L. Leocani, *Optical Coherence Tomography and Visual Evoked Potentials as Prognostic and Monitoring Tools in Progressive Multiple Sclerosis.* Front Neurosci, 2021. **15**: p. 692599.
47. Bennett, J.L., *Optical Coherence Tomography, Retinal Atrophy, and Neurodegeneration in Progressive Multiple Sclerosis: Sprinting to the Finish.* Neurology, 2023. **101**(10): p. 420-421.
48. Wattjes, M.P., et al., *2021 MAGNIMS-CMSC-NAIMS consensus recommendations on the use of MRI in patients with multiple sclerosis.* Lancet Neurol, 2021. **20**(8): p. 653-670.
49. Jiang, H., S. Delgado, and J. Wang, *Advances in ophthalmic structural and functional measures in multiple sclerosis: do the potential ocular biomarkers meet the unmet needs?* Curr Opin Neurol, 2021. **34**(1): p. 97-107.
50. Outteryck, O., et al., *Optical coherence tomography for detection of asymptomatic optic nerve lesions in clinically isolated syndrome.* Neurology, 2020. **95**(6): p. e733-e744.
51. de Seze, J., *Inflammatory Optic Neuritis: From Multiple Sclerosis to Neuromyelitis Optica.* Neuroophthalmology, 2013. **37**(4): p. 141-145.
52. Minakaran, N., et al., *Optical coherence tomography (OCT) in neuro-ophthalmology.* Eye (Lond), 2021. **35**(1): p. 17-32.
53. Delazer, L., et al., *Association between retinal thickness and disease characteristics in adult epilepsy: A cross-sectional OCT evaluation.* Epilepsia Open, 2024. **9**(1): p. 236-249.
54. Schworm, B., et al., *Age-dependent retinal neuroaxonal degeneration in children and adolescents with Leber hereditary optic neuropathy under idebenone therapy.* Eur J Neurol, 2023. **30**(8): p. 2525-2533.
55. Lotz-Havla, A.S., et al., *Optical Coherence Tomography: Retinal Imaging Contributes to the Understanding of Brain Pathology in Classical Galactosemia.* J Clin Med, 2023. **12**(5).
56. Brendel, M., et al., *[(18)F]-THK5351 PET Correlates with Topology and Symptom Severity in Progressive Supranuclear Palsy.* Front Aging Neurosci, 2017. **9**: p. 440.
57. Hoffmann, G.F. and B. Assmann, *Stoffwechselerkrankungen in der Neurologie*. 2004: Thieme.
58. van Wegberg, A.M.J., et al., *The complete European guidelines on phenylketonuria: diagnosis and treatment.* Orphanet J Rare Dis, 2017. **12**(1): p. 162.
59. van Spronsen, F.J., et al., *Phenylketonuria.* Nat Rev Dis Primers, 2021. **7**(1): p. 36.
60. Blau, N., et al., *Diagnosis, classification, and genetics of phenylketonuria and tetrahydrobiopterin (BH4) deficiencies.* Mol Genet Metab, 2011. **104 Suppl**: p. S2-9.
61. Blau, N., F.J. van Spronsen, and H.L. Levy, *Phenylketonuria.* Lancet, 2010. **376**(9750): p. 1417-27.
62. Ney, D.M., R.D. Blank, and K.E. Hansen, *Advances in the nutritional and pharmacological management of phenylketonuria.* Curr Opin Clin Nutr Metab Care, 2014. **17**(1): p. 61-8.
63. Hennermann, J.B. and J.B. Hennermann, *Neue Erkenntnisse und Strategien in der Behandlung der Phenylketonurie*. 2014: Südwestdeutscher Verlag für Hochschulschriften.
64. Pilotto, A., et al., *Phenylalanine Effects on Brain Function in Adult Phenylketonuria.* Neurology, 2021. **96**(3): p. e399-e411.

65. Hawks, Z., et al., *White and gray matter brain development in children and young adults with phenylketonuria.* Neuroimage Clin, 2019. **23**: p. 101916.
66. Anderson, P.J. and V. Leuzzi, *White matter pathology in phenylketonuria.* Mol Genet Metab, 2010. **99 Suppl 1**: p. S3-9.
67. Hood, A., et al., *Prolonged exposure to high and variable phenylalanine levels over the lifetime predicts brain white matter integrity in children with phenylketonuria.* Mol Genet Metab, 2015. **114**(1): p. 19-24.
68. Albrecht, P., et al., *Retinal neurodegeneration in Wilson's disease revealed by spectral domain optical coherence tomography.* PLoS One, 2012. **7**(11): p. e49825.
69. Havla, J., et al., *Retinal axonal degeneration in Niemann-Pick type C disease.* J Neurol, 2020. **267**(7): p. 2070-2082.

10. Danksagung

Durch mein langes Interesse an der neurologischen Forschung, sowie meiner Arbeit als studentische Hilfkraft in der Klinik für Neuroimmunologie, war ich hochmotiviert meine Promotion in der Neuroimmunologie zu realisieren. Fünf Jahre lang habe ich in Großhadern und Berg am Starnberg für meine Dissertation gearbeitet.

An dieser Stelle möchte ich allen beteiligten Personen danken. Besonderer Dank gilt meinem Doktorvater, PD Dr. Joachim Havla, für die Zusammenarbeit in diesen Jahren, sowie meinen anderen Betreuern, Frau Professor Tania Kümpfel, Leiterin der neuroimmunologischen Ambulanz in Großhadern, und Herr Professor Ingo Kleiter, ärztlicher Leiter der Marianne-Strauss-Klinik in Berg. Dank der Bereitstellung einer MS-Kohorte der Marianne-Strauss-Klinik war diese Promotion möglich. Mein Dank gilt auch Frau Dr. Amelie Lotz-Havla vom Dr. von Haunerschen Kinderspital. Vielen Dank auch an Jonathan Gernert für die Zusammenarbeit an unserer Veröffentlichung.

Des Weiteren bedanke ich mich bei den Mitarbeiterinnen der OCT-Ambulanzen in der Klinik für Neuorimmunologie in Großhadern sowie in der Marianna-Strauss-Klinik, die Zusammenarbeit war immer unkompliziert und hat mir viel Freude bereitet.

Eine Dissertation abzuschließen, erfordert oft viel Geduld und die Fähigkeit, Frustrationen zu bewältigen. Mein tiefster Dank gilt meinen Eltern und meinen Freunden. Ihr hattet nicht nur immer ein offenes Ohr für mich, sondern seid oft die Quelle meiner Motivation gewesen und habt mich ermutigt, inspiriert und unterstützt, dieses Projekt zu vollenden.